

Analysis of Dalitz decays with intrinsic parity violating interactions in resonance chiral perturbation theory

Daiji Kimura*

National Institute of Technology, Ube College, Ube Yamaguchi 755-8555, Japan

Takuya Morozumi† and Hiroyuki Umeeda‡

*Graduate School of Science, Core of Research for the Energetic Universe,
Hiroshima University, Higashi-Hiroshima 739-8526, Japan*

(Dated: September 30, 2016)

Abstract

Transition form factors and partial decay widths are investigated for Dalitz decays of $V \rightarrow Pl^+l^-$ and $P \rightarrow \gamma l^+l^-$ ($V = 1^-, P = 0^-$) in a model of resonance chiral perturbation theory. The differential decay width of $P \rightarrow \pi^+\pi^-\gamma$ and the partial widths of $V \rightarrow 3P, V \rightarrow P\gamma, \eta' \rightarrow V\gamma, \phi \rightarrow \omega\pi^0$ and $P \rightarrow 2\gamma$ are also analyzed. The model contains octet and singlet fields as representation of SU(3). 1-loop order counter terms are introduced, based on the discussion of superficial degree of divergence. Intrinsic parity violating interactions are considered with singlet fields. We give the result of numerical analysis, and find a parameter region consistent with experimental data of transition form factors for $V \rightarrow Pl^+l^-$. Predictions of the model are presented for transition form factors of $P \rightarrow \gamma l^+l^-$, differential decay width of $P \rightarrow \pi^+\pi^-\gamma$ and so forth. Furthermore, in the vicinity of resonance regions, the transition form factors of $\phi \rightarrow \pi^0 l^+l^-$ and $\eta' \rightarrow \gamma l^+l^-$ are analyzed with taking account of the contribution from intermediate ρ and ω .

PACS numbers: 12.39.Fe, 13.20.-v, 14.40.Aq

* E-mail: kimurad@ube-k.ac.jp

† E-mail: morozumi@hiroshima-u.ac.jp

‡ E-mail: umeeda@theo.phys.sci.hiroshima-u.ac.jp

I. INTRODUCTION

Decays of light hadrons play a crucial role to investigate low-energy behavior of QCD, and are measured extensively in experiments. One can verify the validity of QCD effective theories through experimental data of hadronic decay width. In particular, Dalitz decays such as $P \rightarrow \gamma l^+ l^-$ and $V \rightarrow P l^+ l^-$ yield rich resources as hadronic observables. As a recent result, high-precision data of transition form factors (TFFs) for $\omega \rightarrow \pi^0 \mu^+ \mu^-$ and $\eta \rightarrow \mu^+ \mu^- \gamma$ are obtained by NA60 collaboration[1] in proton-nucleus (p-A) collisions. Moreover, the first measurement of the branching ratio and the TFF of $\eta' \rightarrow \gamma e^+ e^-$ has been carried out by BES III collaboration[2].

To describe dynamics of light hadrons, resonance chiral perturbation theory (R χ PT) is extensively used. In R χ PT, vector mesons are included as the resonance fields [3–5]. This effective dynamics is applicable to a variety of phenomena, e.g., hadronic decays of τ . In our study, 1-loop order counter terms, which correspond to $O(p^4)$, are introduced in the framework including vector mesons. The form of interaction terms is specified with power counting of superficial degree of divergence.

In processes such as $P \rightarrow 2\gamma$ and radiative decays of $V \rightarrow P\gamma$, intrinsic parity (IP)[6] is violated. It is well-known that intrinsic parity violation (IPV) in R χ PT is categorized as two types: The first one is the Wess-Zumino-Witten (WZW) term, which results from quantum anomaly of SU(3) symmetry[7, 8]. The second one comes from the presence of resonance fields of vector meson, as originally suggested in the framework of hidden local symmetry (HLS)[9, 10].

In this paper, the observables of IP violating decays such as the TFFs and the partial widths of light hadrons are analyzed in a model of R χ PT. For the HLS model, a numerical result for IP violating decay widths is given in Refs.[11, 12], with SU(3) breaking effect in IP violating interactions. Numerical analysis of the TFFs are given in Refs.[13–16]. We adopt the model which contains chiral octet and singlet as representation of SU(3). After diagonalizing the mass matrix of vector mesons, mass eigenstates play the role as resonance fields of $\rho(770)$, $\omega(782)$ and $\phi(1020)$. 1-loop correction to the self-energy for vector mesons is calculated, and it is shown that kinetic mixing effect gives rise to contribution to the decay width of $V \rightarrow PP$. Parameters in the model, i.e., values of the $\rho\pi\pi$ coupling, mixing matrix elements of vector mesons, etc., are fixed to realize the minimum of χ^2 for experimental data

of the masses and decay widths of ρ, ω and ϕ . As for IP violating interactions, operators with SU(3) singlet fields are introduced. Inclusion of the singlet-induced IP violating operators plays an important role in the framework of octet+singlet scheme, typically for $\eta' \rightarrow 2\gamma$. Formulae for partial width and its distribution are given for the IP violating decays, and model prediction for the TFFs is presented in this work. To estimate the parameter ranges in the model, the χ^2 fitting is performed with data obtained in experiments. We find a parameter region which is consistent with experimental values for the TFFs of $V \rightarrow Pl^+l^-$. Using the estimated parameter ranges, we give predictions for (1) the partial decay widths of $P \rightarrow \gamma l^+l^-, P \rightarrow \pi^+\pi^-\gamma, V \rightarrow Pl^+l^-, V \rightarrow P\pi^+\pi^-$ and $\phi \rightarrow \omega\pi^0$, (2) the electromagnetic TFFs of $P \rightarrow \gamma l^+l^-$, (3) the differential decay widths of $P \rightarrow \pi^+\pi^-\gamma$ and (4) the TFFs of $\rho^0 \rightarrow \pi^0 l^+l^-, \rho^0 \rightarrow \eta l^+l^-, \omega \rightarrow \eta l^+l^-$ and $\phi \rightarrow \eta' l^+l^-$. As discussed in the latter part of the paper, the TFFs for $\phi \rightarrow \pi^0 l^+l^-$ and $\eta' \rightarrow \gamma l^+l^-$ have a peak region around which di-lepton invariant mass is close to the masses of ρ and ω .

Remaining part of this paper is organized as follows: In Sec.II, the model of R χ PT is proposed and 1-loop ordered interactions are introduced with SU(3) octets and singlets. The masses of vector mesons, kinetic mixing correction to the widths of vector mesons, the mixing between photon and vector mesons and the mixing matrix of pseudoscalars are analyzed. The ratio of decay constants for pseudoscalars with 1-loop correction is also given. Intrinsic parity violating parts in Lagrangian are given, taking account of chiral singlet fields in Sec.III, and the formulae of (differential) decay width for light hadrons are obtained. The results of numerical analysis are presented in Sec.IV so that values of parameters are fixed with fitting data of the masses and the widths of vector mesons. For coefficients of IP violating interaction, we estimate the parameter range which is consistent with experimental data of the TFFs in $V \rightarrow Pl^+l^-$. The predictions for decay widths and distributions are also given. Finally, Sec.V is dedicated to summary and discussion.

II. THE MODEL WITH SU(3) OCTETS AND SINGLETS

In this section, we introduce a model of chiral Lagrangian with vector mesons [18]. In this paper, we extend the previous one so that it includes ϕ meson and electromagnetic mass

of pseudoscalar mesons as follows,

$$\mathcal{L}_\chi = \mathcal{L}_P + \mathcal{L}_V + \mathcal{L}_c, \quad (1)$$

$$\begin{aligned} \mathcal{L}_P = & \frac{f^2}{4} \text{Tr}(D_\mu U D^\mu U^\dagger) + B \text{Tr}[M(U + U^\dagger)] + C \text{Tr} Q U Q U^\dagger \\ & + \frac{1}{2} \partial_\mu \eta_0 \partial^\mu \eta_0 - \frac{1}{2} M_{00}^2 \eta_0^2 - i g_{2p} \eta_0 \text{Tr}[M(U - U^\dagger)], \end{aligned} \quad (2)$$

$$\begin{aligned} \mathcal{L}_V = & -\frac{1}{2} \text{Tr} F_V^{\mu\nu} F_{V\mu\nu} + M_V^2 \text{Tr} \left(V_\mu - \frac{\alpha_\mu}{g} \right)^2 + g_{1V} \phi_\mu^0 \text{Tr} \left\{ \left(V^\mu - \frac{\alpha^\mu}{g} \right) \left(\frac{\xi M \xi + \xi^\dagger M \xi^\dagger}{2} \right) \right\} \\ & - \frac{1}{4} F_{V\mu\nu}^0 F_V^{0\mu\nu} + \frac{1}{2} M_{0V}^2 \phi_\mu^0 \phi^{0\mu}, \end{aligned} \quad (3)$$

where

$$\alpha_\mu = \frac{1}{2i} (\xi^\dagger D_{L\mu} \xi + \xi D_{R\mu} \xi^\dagger), \quad (4)$$

$$D_{L(R)\mu} = \partial_\mu + i A_{L(R)\mu}, \quad (5)$$

$$U = \xi^2 = \exp \left(\frac{2i\pi}{f} \right), \quad (6)$$

$$D_\mu U = \partial_\mu U + i A_{L\mu} U - i U A_{R\mu}, \quad (7)$$

$$M = \text{diag}(m_u, m_d, m_s), \quad (8)$$

$$F_{V\mu\nu} = \partial_\mu V_\nu - \partial_\nu V_\mu + ig[V_\mu, V_\nu], \quad (9)$$

$$F_{V\mu\nu}^0 = \partial_\mu \phi_\nu - \partial_\nu \phi_\mu, \quad (10)$$

$$Q = \text{diag} \left(\frac{2}{3}, -\frac{1}{3}, -\frac{1}{3} \right). \quad (11)$$

The Lagrangian is divided into three parts in Eq.(1), which consist of the parts of pseudoscalars, vector mesons, and 1-loop order counter terms. As fields of pseudoscalar, the octet matrix and the singlet field are contained in Eq.(2). η_0 is $U(1)_A$ pseudoscalar and its mass is given as M_{00} . The term denoted as $C \text{Tr} Q U Q U^\dagger$ in Eq.(2) is the electromagnetic correction to chiral perturbation theory (χ PT). This term describes the effect of virtual photon [19], and affects the mass of the charged pseudoscalar. Vector mesons are introduced as SU(3) octet and singlet in Eq.(3). Vector meson matrix for octet is denoted by V_μ , and its mass is given as M_V , while the field ϕ_μ^0 denotes SU(3) singlet vector meson.

In the following, we present how 1-loop counter terms given as \mathcal{L}_c are introduced for chiral Lagrangian with vector mesons and pseudoscalar singlet. The form of 1-loop counter terms depends on the tree level Lagrangian and is obtained with power counting of the superficial degree of divergence in the loop calculation. The tree level Lagrangian is constructed based

on the expansion with respect to derivatives and chiral SU(3) breaking. The Lagrangian includes either the second derivatives or an insertion of chiral SU(3) breaking. The interaction Lagrangian which satisfies such criteria is extracted from Eqs.(2, 3),

$$\begin{aligned}\mathcal{L}_0 = & \frac{f^2}{4} \text{Tr} D_\mu U D^\mu U^\dagger + M_V^2 \text{Tr} \left(V_\mu - \frac{\alpha_\mu}{g} \right)^2 \\ & + B \text{Tr}(M(U + U^\dagger)) - i g_{2p} \eta_0 \text{Tr}(M(U - U^\dagger)).\end{aligned}\quad (12)$$

Note that \mathcal{L}_0 does not include the parts which are written only with vector mesons and singlet pseudoscalars. With \mathcal{L}_0 , the divergent parts of the 1-loop correction is extracted and the counter terms are given in Eq.(A1). As proven in App.B, the counter terms satisfy the power counting rule, which enables us to specify the structure of them. Based on the discussion, in Eq.(1), we have included a singlet-octets vector mesons mixing term as a finite counter term.

The counter terms for the self-energy of vector mesons and $V - \gamma$ mixing can be summarized as the effective counter terms [18],

$$\begin{aligned}\mathcal{L}_c^{eff} = & -\frac{1}{2} Z_V^{(1)} \text{Tr}(\mathcal{F}_{V\mu\nu} \mathcal{F}_V^{\mu\nu}) \\ & + C_1 \text{Tr} \left[\frac{\xi \chi \xi + \xi^\dagger \chi^\dagger \xi^\dagger}{2} \left(V_\mu - \frac{\alpha_\mu}{g} \right)^2 \right] + C_2 \text{Tr} \left(\frac{\xi \chi \xi + \xi^\dagger \chi^\dagger \xi^\dagger}{2} \right) \text{Tr} \left[\left(V_\mu - \frac{\alpha_\mu}{g} \right)^2 \right] \\ & + C_4 \text{Tr} \mathcal{F}_V^{\mu\nu} (F_{L\mu\nu}^0 + F_{R\mu\nu}^0),\end{aligned}\quad (13)$$

$$\chi = \frac{4BM}{f^2}.\quad (14)$$

where all the field strength are Abelian part defined by, $\mathcal{F}_{V\mu\nu} = \partial_\mu V_\nu - \partial_\nu V_\mu$ and $F_{L(R)\mu\nu}^0 = \partial_\mu A_{L(R)\nu} - \partial_\nu A_{L(R)\mu}$. $Z_V^{(1)}$ and C_i ($i = 1, 2, 4$) are renormalization constants and they are written in terms of the coefficients in Eq.(A1),

$$\begin{aligned}Z_V^{(r)(1)} = & K_3^{(r)} (g_{\rho\pi\pi})_{\text{tr}}^2, \quad C_1^{(r)} = 2K_4^{(r)} (g_{\rho\pi\pi})_{\text{tr}}^2, \\ C_2^{(r)} = & 2K_5^{(r)} (g_{\rho\pi\pi})_{\text{tr}}^2, \quad C_4^{(r)} = -\frac{(g_{\rho\pi\pi})_{\text{tr}}}{2} \left(K_2^{(r)} - K_3^{(r)} \frac{M_V^2}{2g^2 f^2} \right),\end{aligned}\quad (15)$$

where $(g_{\rho\pi\pi})_{\text{tr}} = M_V^2/(2gf^2)$ denotes a tree level vertex for $\rho\pi\pi$ coupling. Hereafter, we use approximation of $(g_{\rho\pi\pi})_{\text{tr}} \simeq M_V^2/(2gf_\pi^2) = g_{\rho\pi\pi}$ since their difference is negligible in 1-loop order calculation. The coefficients of the effective counter terms in Eq.(15) include the divergent part and the finite part. The finite parts are denoted with suffix (r) . Both divergent and finite parts of K_i are recorded in Eq.(A4).

A. Neutral vector meson sector (ρ, ω, ϕ)

In this subsection, we diagonalize the mass matrix for neutral vector mesons and obtain the mass eigenstates which correspond to (ρ, ω, ϕ) . The mixing matrix between $(\rho_0, \omega_8, \phi_0)$ and mass eigenstates determines the interaction among the physical states. The inverse propagator for the vector mesons is,

$$\frac{1}{2} V^{\mu I} D_{\mu\nu IJ}^{-1} V^{\nu J}, \quad (16)$$

where V^I denotes the eigenstate for the mass matrix, $V_\mu^T = (V_\mu^1, V_\mu^2, V_\mu^3) = (\rho_\mu, \omega_\mu, \phi_\mu)$. The mixing matrix O_V relates the mass eigenstates to SU(3) basis in the following,

$$V_\mu^0 = \begin{pmatrix} \rho_\mu^0 \\ \omega_\mu^8 \\ \phi_\mu^0 \end{pmatrix} = O_V V_\mu. \quad (17)$$

In Eq.(16), $D_{\mu\nu}^{-1} = O_V^T D_{\mu\nu}^{0-1} O_V$ contains the self-energy correction,

$$D_{\mu\nu}^{0-1} = g_{\mu\nu} \begin{pmatrix} M_\rho^2 & M_{V\rho 8}^2 & M_{V0\rho}^2 \\ M_{V\rho 8}^2 & M_{V88}^2 & M_{V08}^2 \\ M_{V0\rho}^2 & M_{V08}^2 & M_{0V}^2 \end{pmatrix} + Q_{\mu\nu} \begin{pmatrix} \delta B_\rho(Q^2) & \delta B_{\rho 8}(Q^2) & 0 \\ \delta B_{\rho 8}(Q^2) & \delta B_{88}(Q^2) & 0 \\ 0 & 0 & 1 \end{pmatrix}, \quad (18)$$

$$Q_{\mu\nu} = Q_\mu Q_\nu - g_{\mu\nu} Q^2, \quad (19)$$

$$\delta B_\rho = Z_V^r(\mu) + g_{\rho\pi\pi}^2 (4M_\pi^r + M_{K^+}^r + M_{K^0}^r), \quad (20)$$

$$\delta B_{\rho 8} = \sqrt{3} g_{\rho\pi\pi}^2 \Delta M_{K^+K^0}^r, \quad (21)$$

$$\delta B_{88} = Z_V^r(\mu) + 3g_{\rho\pi\pi}^2 (M_{K^+}^r + M_{K^0}^r), \quad (22)$$

where $\Delta M_{K^+K^0}^r = M_{K^+}^r - M_{K^0}^r$. In Eqs.(20, 22), Z_V^r denotes the coefficient of kinetic term of octet vector meson defined as $1 + Z_V^{r(1)}$. M_P^r are the loop functions of vector mesons,

$$M_P^r = \frac{1}{12} \left[\left(1 - \frac{4M_P^2}{Q^2} \right) \bar{J}_P - \frac{1}{16\pi^2} \ln \frac{M_P^2}{\mu^2} - \frac{1}{48\pi^2} \right], \quad (23)$$

$$\bar{J}_P = \begin{cases} -\frac{1}{16\pi^2} \sqrt{1 - \frac{4M_P^2}{Q^2}} \ln \frac{1 + \sqrt{1 - \frac{4M_P^2}{Q^2}}}{1 - \sqrt{1 - \frac{4M_P^2}{Q^2}}} + \frac{1}{8\pi^2} + i \frac{1}{16\pi} \sqrt{1 - \frac{4M_P^2}{Q^2}}, & (Q^2 \geq 4M_P^2), \\ \frac{1}{8\pi^2} \left(1 - \sqrt{\frac{4M_P^2}{Q^2}} - 1 \arctan \frac{1}{\sqrt{\frac{4M_P^2}{Q^2} - 1}} \right), & (Q^2 \leq 4M_P^2), \end{cases}$$

where μ is a renormalization scale. In the numerical analysis, we fix it as $\mu = m_{K^{*+}}$. The elements in the mass matrix (18) are given by,

$$M_\rho^2 = M_V^2 + C_1^r M_\pi^2 + C_2^r (2\bar{M}_K^2 + M_\pi^2) - 4g_{\rho\pi\pi}^2 \left(\mu_\pi + \frac{\bar{\mu}_K}{2} \right) f^2, \quad (24)$$

$$M_{V88}^2 = M_V^2 + C_1^r \frac{4\bar{M}_K^2 - M_\pi^2}{3} + C_2^r (2\bar{M}_K^2 + M_\pi^2) - 6g_{\rho\pi\pi}^2 \bar{\mu}_K f^2, \quad (25)$$

$$M_{V\rho8}^2 = \frac{1}{\sqrt{3}} \{ C_1^r \Delta_{K^+K^0} - 3g_{\rho\pi\pi}^2 \Delta\mu_K f^2 \}, \quad (26)$$

$$M_{V0\rho}^2 = \frac{\hat{g}_{1V}}{4} \Delta_{K^+K^0}, \quad (27)$$

$$M_{V08}^2 = -\frac{\hat{g}_{1V}}{2\sqrt{3}} \Delta_{K\pi}, \quad (28)$$

with

$$\mu_P = \frac{M_P^2}{32\pi^2 f^2} \ln \left(\frac{M_P^2}{\mu^2} \right), \quad \bar{\mu}_K = \frac{\mu_{K^+} + \mu_{K^0}}{2}, \quad (29)$$

$$\bar{M}_K^2 = \frac{M_{K^+}^2 + M_{K^0}^2}{2}, \quad M_\pi^2 = M_{\pi^+}^2 = M_{\pi^0}^2, \quad (30)$$

$$\hat{g}_{1V} = \frac{f^2 g_{1V}}{B}, \quad \Delta\mu_K = \mu_{K^+} - \mu_{K^0}, \quad (31)$$

$$\Delta_{PQ} = M_P^2 - M_Q^2, \quad \Delta_{K\pi} = \bar{M}_K^2 - M_\pi^2. \quad (32)$$

We calculate the mass of the neutral vector mesons, ρ, ω and ϕ . The first term in Eq.(18) is diagonalized as,

$$D_{\mu\nu}^{-1} = g_{\mu\nu} \mathcal{M}^2 + \delta B_V(Q^2) Q_{\mu\nu}, \quad (33)$$

$$\mathcal{M}^2 = \text{diag}(\mathcal{M}_1^2, \mathcal{M}_2^2, \mathcal{M}_3^2), \quad (34)$$

where $\delta B_V(Q^2)$ is a 3×3 matrix,

$$\delta B_V(Q^2) = O_V^T \delta B(Q^2) O_V. \quad (35)$$

The propagator for the neutral vector mesons is denoted as,

$$D^{\mu\nu} = g^{\mu\nu} D_0 + Q^\mu Q^\nu D_L, \quad (36)$$

$$D_0 = (\mathcal{M}^2 - Q^2 \delta B_V)^{-1}, \quad (37)$$

$$D_L = \frac{1}{Q^2} \left(\frac{1}{\mathcal{M}^2} - \frac{1}{\mathcal{M}^2 - Q^2 \delta B_V} \right). \quad (38)$$

In the following, we expand the propagator in Eq.(36) with respect to the off-diagonal parts of δB_V ,

$$(D_{\mu\nu})_{IJ} = \begin{cases} g_{\mu\nu} - \frac{Q_\mu Q_\nu}{\mathcal{M}_I^2} \delta B_{VI} \\ \frac{\mathcal{M}_I^2 - Q^2 \delta B_{VI}}{\mathcal{M}_I^2 - Q^2 \delta B_{VI}}, & (I = J) \\ -Q_{\mu\nu} \frac{1}{\mathcal{M}_I^2 - Q^2 \delta B_{VI}} \delta B_{VIJ} \frac{1}{\mathcal{M}_J^2 - Q^2 \delta B_{VJ}}, & (I \neq J) \end{cases} \quad (39)$$

where $I, J = 1, 2, 3$ and δB_{VI} denotes the diagonal part in the matrix in Eq.(35). If one neglects the off-diagonal parts of δB_V , the above propagator becomes diagonal matrix given in the first line in Eq.(39). The pole mass squared is defined as the momentum squared where the real part of the denominator of the propagator vanishes in the following as,

$$\mathcal{M}_I^2 - m_I^2 \text{Re} \delta B_{VI}(m_I^2) = 0. \quad (40)$$

The denominator of the propagator in Eq.(39) is expanded in the vicinity of the pole mass,

$$\begin{aligned} \mathcal{M}_I^2 - Q^2 \text{Re} \delta B_{VI}(Q^2) &= m_I^2 \text{Re} \delta B_{VI}(m_I^2) - Q^2 \text{Re} \delta B_{VI}(Q^2) \\ &\simeq (m_I^2 - Q^2) \frac{dQ^2 \text{Re} \delta B_{VI}(Q^2)}{dQ^2} \Big|_{Q^2=m_I^2}. \end{aligned} \quad (41)$$

We define the wave function renormalization of neutral vector meson,

$$Z_I^{-1} = \frac{dQ^2 \text{Re} \delta B_{VI}(Q^2)}{dQ^2} \Big|_{Q^2=m_I^2} = \text{Re} \delta B_{VI}(m_I^2) + m_I^2 \frac{d \text{Re} \delta B_{VI}(Q^2)}{dQ^2} \Big|_{Q^2=m_I^2}. \quad (42)$$

Thus, in the vicinity of the pole mass, the propagator takes the following form,

$$(D_{\mu\nu})_{II} \simeq Z_I \frac{g_{\mu\nu} - \frac{Q_\mu Q_\nu}{m_I^2} \left(1 + i \frac{\text{Im} \delta B_{VI}(m_I^2)}{\text{Re} \delta B_{VI}(m_I^2)} \right)}{m_I^2 - Q^2 - i m_I \Gamma_I}, \quad (43)$$

where the definitions of the pole mass and width are given as,

$$m_I^2 = \frac{\mathcal{M}_I^2}{\text{Re} \delta B_{VI}(m_I^2)}, \quad (44)$$

$$\Gamma_I = m_I Z_I \text{Im} \delta B_{VI}(m_I^2). \quad (45)$$

B. Kinetic mixing of the vector mesons

To evaluate the partial decay width for $V^I \rightarrow PP$, kinetic mixing in the decay process, i.e., $V^I \rightarrow V^J \rightarrow PP$, should be taken into account. The renormalized fields are related

with the bare fields through the wave function renormalization in Eq.(42) as,

$$\begin{pmatrix} \rho_\mu \\ \omega_\mu \\ \phi_\mu \end{pmatrix} = \begin{pmatrix} \sqrt{Z_1} & 0 & 0 \\ 0 & \sqrt{Z_2} & 0 \\ 0 & 0 & \sqrt{Z_3} \end{pmatrix} \begin{pmatrix} \rho_\mu^R \\ \omega_\mu^R \\ \phi_\mu^R \end{pmatrix}. \quad (46)$$

Using the renormalized fields, we can express the kinetic mixing terms,

$$\mathcal{L}_{\text{KM}} = \frac{1}{2} \begin{pmatrix} \rho_\mu^R & \omega_\mu^R & \phi_\mu^R \end{pmatrix} Q^{\mu\nu} \begin{pmatrix} 0 & \delta B_{V12} & \delta B_{V13} \\ \delta B_{V12} & 0 & \delta B_{V23} \\ \delta B_{V13} & \delta B_{V23} & 0 \end{pmatrix} \begin{pmatrix} \rho_\nu^R \\ \omega_\nu^R \\ \phi_\nu^R \end{pmatrix}. \quad (47)$$

In the kinetic mixing terms, we set the wave function renormalization $Z_I = 1$, since δB_{VIJ} ($I \neq J$) is 1-loop order contribution. For example, we consider $V^I \rightarrow \pi^+\pi^-$ decays. Using coupling of the neutral vector mesons to $\pi^+\pi^-$,

$$\mathcal{L}_\chi|_{V^I\pi^+\pi^-} = 2ig_{\rho\pi\pi}\Pi_I V_\mu^I \left(\pi^+ \overleftrightarrow{\partial}^\mu \pi^- \right), \quad (48)$$

$$\Pi_I = \frac{O_{V1I}}{2} + \frac{\hat{g}_{1V}}{8} \frac{M_{K^+}^2 - M_{K^0}^2}{M_V^2} O_{V3I}, \quad (49)$$

we have the T -matrix element including the kinetic mixing effects,

$$\begin{aligned} T^I &= -2g_{\rho\pi\pi}(p_+ + p_-) \cdot \epsilon \left(\Pi_I \sqrt{Z_I} + \sum_{J \neq I} \Pi_J \frac{m_I^2}{\mathcal{M}_J^2 - m_I^2 \delta B_{VJ}(m_I^2)} \delta B_{VJI} \right) \\ &\simeq -2g_{\rho\pi\pi}(p_+ + p_-) \cdot \epsilon \left(\Pi_I \sqrt{Z_I} - \sum_{J \neq I} \Pi_J \frac{m_I^2}{m_I^2 - m_J^2 - im_J \Gamma_J} \delta B_{VJI} \right), \end{aligned} \quad (50)$$

where p_+ and p_- are the momenta of π^+ and π^- , respectively. The second term denotes the kinetic mixing effects for $V^I \rightarrow V^J \rightarrow \pi^+\pi^-$ decay process. In the first line in Eq.(50), \mathcal{M}_J ($J = 1, 2, 3$) is the eigenvalue for the vector meson mass matrix, which differs from the physical masses, m_ρ, m_ω or m_ϕ . We take Γ_J as the experimental value of total widths of ρ, ω and ϕ . Momentum dependence on the imaginary part of δB_V is ignored in the second line in Eq.(50). Thus, the partial widths for $\omega \rightarrow \pi^+\pi^-$, $\phi \rightarrow K^+K^-$ and $\phi \rightarrow K^0\bar{K}^0$ are described to be,

$$\Gamma[V^I \rightarrow PP] = \frac{m_I |g_{VPP}^{\text{eff}}|^2}{12\pi} \left(1 - \frac{4M_P^2}{m_I^2} \right)^{\frac{3}{2}}. \quad (51)$$

Here, g_{VPP}^{eff} indicates the tree level VPP coupling containing the kinetic mixing effect. g_{VPP}^{eff} is given as,

$$g_{\omega\pi^+\pi^-}^{\text{eff}} \simeq g_{\rho\pi\pi} \left[\sqrt{Z_2} \Pi_2 - m_\omega^2 \sum_{J=\rho,\phi} \Pi_J \frac{\delta B_{VJ2}}{m_\omega^2 - m_J^2 - im_J \Gamma_J} \right], \quad (52)$$

$$g_{\phi K^+ K^-}^{\text{eff}} \simeq g_{\rho\pi\pi} \left(\frac{f_\pi}{f_K} \right)^2 \left[\sqrt{Z_3} \Pi_3^{K^+} - m_\phi^2 \sum_{J=\rho,\omega} \Pi_J^{K^+} \frac{\delta B_{VJ3}}{m_\phi^2 - m_J^2 - im_J \Gamma_J} \right], \quad (53)$$

$$g_{\phi K^0 \bar{K}^0}^{\text{eff}} \simeq g_{\rho\pi\pi} \left(\frac{f_\pi}{f_K} \right)^2 \left[\sqrt{Z_3} \Pi_3^{K^0} - m_\phi^2 \sum_{J=\rho,\omega} \Pi_J^{K^0} \frac{\delta B_{VJ3}}{m_\phi^2 - m_J^2 - im_J \Gamma_J} \right], \quad (54)$$

$$\Pi_I^{K^+} = \frac{O_{V1I}}{4} + \frac{\sqrt{3}}{4} O_{V2I} + \frac{\hat{g}_{1V}(M_{\pi^+}^2 - M_{K^0}^2)}{8M_V^2} O_{V3I}, \quad (55)$$

$$\Pi_I^{K^0} = -\frac{O_{V1I}}{4} + \frac{\sqrt{3}}{4} O_{V2I} + \frac{\hat{g}_{1V}(M_{\pi^+}^2 - M_{K^+}^2)}{8M_V^2} O_{V3I}, \quad (56)$$

$$\Pi_1 = \Pi_\rho, \quad \Pi_3 = \Pi_\phi, \quad \Pi_1^{K^{0(+)}} = \Pi_\rho^{K^{0(+)}} , \quad \Pi_2^{K^{0(+)}} = \Pi_\omega^{K^{0(+)}} . \quad (57)$$

C. Mixing between photon and vector meson

In this subsection, the mixing between photon and vector mesons is analyzed. The contributing diagrams for $V - A$ mixing in 1-loop order are exhibited in Fig.II.1. The $V - \gamma$

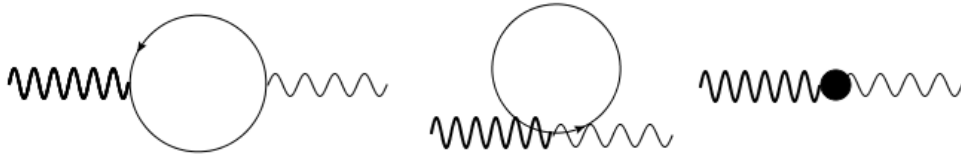


FIG. II.1. Feynman diagrams for the two-point function of the mixing of photon and vector meson.

Wavy lines imply vector meson while bold wavy lines indicate the vector mesons.

conversion vertex is denoted as,

$$\mathcal{L}_\chi|_{V\gamma} = V_\mu^{0I} \Pi^{\mu\nu V^{0I}A} A_\nu = V_\mu^I \Pi^{\mu\nu V^I A} A_\nu, \quad (58)$$

$$\Pi_{\mu\nu}^{V^I A} = O_V^T \Pi_{\mu\nu}^{V^{0I} A}. \quad (59)$$

In the basis of $SU(3)$, the two-point functions in the l.h.s. of Eq.(58) are given as,

$$\Pi_{\mu\nu}^{V^{0I}A} = eg_{\mu\nu}\Pi^{V^{0I}A} + eQ_{\mu\nu}\Pi_T^{V^{0I}A}, \quad (60)$$

$$\begin{aligned} \Pi^{\rho_0 A} = \frac{1}{g} \left\{ -M_V^2 + 4g_{\rho\pi\pi}^2 \left(\mu_\pi + \frac{\mu_{K^+}}{2} \right) f^2 \right. \\ \left. - C_1^r \left(M_\pi^2 + \frac{\Delta_{K^+K^0}}{3} \right) - C_2^r (2\bar{M}_K^2 + M_\pi^2) \right\}, \end{aligned} \quad (61)$$

$$\Pi_T^{\rho_0 A} = g_{\rho\pi\pi} \left(1 - \frac{M_V^2}{2g^2 f^2} \right) (4M_\pi^r + 2M_{K^+}^r) - 2C_4^r, \quad (62)$$

$$\begin{aligned} \Pi^{\omega_8 A} = \frac{1}{\sqrt{3}g} \left\{ -M_V^2 + 6g_{\rho\pi\pi}^2 \mu_{K^+} f^2 \right. \\ \left. - C_1^r \left(\frac{4\bar{M}_K^2 - M_\pi^2}{3} + \Delta_{K^+K^0} \right) - C_2^r (2\bar{M}_K^2 + M_\pi^2) \right\}, \end{aligned} \quad (63)$$

$$\Pi_T^{\omega_8 A} = 2\sqrt{3}g_{\rho\pi\pi} \left(1 - \frac{M_V^2}{2g^2 f^2} \right) M_{K^+}^r - \frac{2}{\sqrt{3}}C_4^r, \quad (64)$$

$$\Pi^{\phi_0 A} = \frac{\hat{g}_{1V}}{g} \left(\frac{\Delta_{K\pi}}{6} - \frac{\Delta_{K^+K^0}}{4} \right), \quad (65)$$

$$\Pi_T^{\phi_0 A} = 0. \quad (66)$$

One can find that $g^{\mu\nu}$ part in Eq.(60) is related to the matrix elements of the 1-loop corrected neutral vector meson masses in Eqs.(24, 25, 28),

$$\Pi^{V^0 A} = -\frac{1}{g} \begin{pmatrix} M_\rho^2 + \frac{1}{\sqrt{3}}M_{V\rho 8}^2 \\ M_{V\rho 8}^2 + \frac{1}{\sqrt{3}}M_{V88}^2 \\ M_{V0\rho}^2 + \frac{1}{\sqrt{3}}M_{V08}^2 \end{pmatrix}. \quad (67)$$

One can write the two-point functions in Eq.(59),

$$\Pi^{VA} = O_V^T \Pi^{V^0 A} = -\frac{1}{g} \begin{pmatrix} \mathcal{M}_1^2 & 0 & 0 \\ 0 & \mathcal{M}_2^2 & 0 \\ 0 & 0 & \mathcal{M}_3^2 \end{pmatrix} \begin{pmatrix} O_{V11} + \frac{1}{\sqrt{3}}O_{V21} \\ O_{V12} + \frac{1}{\sqrt{3}}O_{V22} \\ O_{V13} + \frac{1}{\sqrt{3}}O_{V23} \end{pmatrix}. \quad (68)$$

The derivation of Eq.(68) is shown in App.D. Thus, the mixing vertices for $V - \gamma$ in Eq.(58) are expressed as,

$$\mathcal{L}_\chi|_{V\gamma} = -\frac{e\mathcal{M}_I^2}{g}\eta_I V_\mu^I A^\mu, \quad (69)$$

$$\eta_I = O_{V1I} + \frac{1}{\sqrt{3}}O_{V2I}. \quad (70)$$

D. Pseudoscalars

In this subsection, the structure of a mixing matrix for pseudoscalars is shown. The result of 1-loop correction to self-energies of pseudoscalars are summarized in App. E for charged particles and in App. F for neutral ones. The basis for an SU(3) eigenstate is related with the mass eigenstate in the following as,

$$\begin{pmatrix} \pi_3 \\ \eta_8 \\ \eta_0 \end{pmatrix} = \sqrt{Z} O \begin{pmatrix} \pi^0 \\ \eta \\ \eta' \end{pmatrix}. \quad (71)$$

where O denotes an orthogonal matrix which diagonalizes the 1-loop corrected mass matrix in Eq.(F10) while \sqrt{Z} is a matrix coming from rescaling of kinetic terms for pseudoscalars. The 1-loop expression of \sqrt{Z} is recorded in Eq.(F7). As shown in Eqs.(F8, F9), \sqrt{Z} contains low energy constants (LECs) which need to be fixed to realize the experimental values. We denote the mixing matrix as,

$$O = \begin{pmatrix} \cos \theta_2 \cos \theta_3 - \cos \theta_1 \sin \theta_2 \sin \theta_3 & \cos \theta_2 \sin \theta_3 + \cos \theta_1 \sin \theta_2 \cos \theta_3 & \sin \theta_1 \sin \theta_2 \\ -\sin \theta_2 \cos \theta_3 - \cos \theta_1 \cos \theta_2 \sin \theta_3 & -\sin \theta_2 \sin \theta_3 + \cos \theta_1 \cos \theta_2 \cos \theta_3 & \sin \theta_1 \cos \theta_2 \\ \sin \theta_1 \sin \theta_3 & -\sin \theta_1 \cos \theta_3 & \cos \theta_1 \end{pmatrix}. \quad (72)$$

1-loop correction to decay constants is taken into account in this work. As stated in App.G, the ratio of the pion decay constant to one for kaon is determined with wave function renormalization of pseudoscalars [18],

$$\frac{f_{K^+}}{f_{\pi^+}} = \sqrt{\frac{Z_{\pi^+}}{Z_{K^+}}} \sim 1 + 4 \frac{M_{K^+}^2 - M_{\pi^+}^2}{f^2} L_5^r + \frac{c}{4} (5\mu_{\pi^+} - 3\mu_{88} - 2\mu_{K^+}), \quad (73)$$

where c is defined as $1 - M_V^2/g^2 f^2$.

III. INTRINSIC PARITY VIOLATION IN R_χPT

In this section, the IP violating operators are introduced. It is well-known that the effect of quantum anomaly yields an IP violating interaction, and the expression of the WZW term is given in Eq.(H1).

Since the resonance fields are contained in the model, IP violating terms are induced by vector mesons. Imposing the charge conjugation (C) symmetry on the IP violating operators, one can obtain,

$$\mathcal{L}_1 = i\epsilon^{\mu\nu\rho\sigma}\text{Tr}[\alpha_{L\mu}\alpha_{L\nu}\alpha_{L\rho}\alpha_{R\sigma} - (R \leftrightarrow L)], \quad (74)$$

$$\mathcal{L}_2 = i\epsilon^{\mu\nu\rho\sigma}\text{Tr}[\alpha_{L\mu}\alpha_{R\nu}\alpha_{L\rho}\alpha_{R\sigma}], \quad (75)$$

$$\mathcal{L}_3 = \epsilon^{\mu\nu\rho\sigma}\text{Tr}[gF_{V\mu\nu}\{\alpha_{L\rho}\alpha_{R\sigma} - (R \leftrightarrow L)\}], \quad (76)$$

$$\mathcal{L}_4 = \frac{1}{2}\epsilon^{\mu\nu\rho\sigma}\text{Tr}[(\hat{F}_{L\mu\nu} + \hat{F}_{R\mu\nu})\{\alpha_{L\rho}, \alpha_{R\sigma}\}], \quad (77)$$

$$\mathcal{L}_5 = \epsilon^{\mu\nu\rho\sigma}F_{V\mu\nu}^0\text{Tr}[\alpha_{L\rho}\alpha_{R\sigma} - (R \leftrightarrow L)], \quad (78)$$

$$\mathcal{L}_6 = \frac{\eta_0}{f}\epsilon^{\mu\nu\rho\sigma}\text{Tr}F_{V\mu\nu}F_{V\rho\sigma}, \quad (79)$$

$$\mathcal{L}_7 = \frac{\eta_0}{f}\epsilon^{\mu\nu\rho\sigma}F_{V\mu\nu}^0F_{V\rho\sigma}^0, \quad (80)$$

$$\mathcal{L}_8 = \epsilon^{\mu\nu\rho\sigma}\text{Tr}(\hat{F}_{L\mu\nu} + \hat{F}_{R\mu\nu})\phi_\rho^0\frac{\alpha_{L\sigma} - \alpha_{R\sigma}}{2}, \quad (81)$$

$$\mathcal{L}_9 = \frac{\eta_0}{f}\epsilon^{\mu\nu\rho\sigma}\text{Tr}(\hat{F}_{L\mu\nu} + \hat{F}_{R\mu\nu})F_{V\rho\sigma}, \quad (82)$$

$$\mathcal{L}_{10} = \frac{\eta_0}{f}\epsilon^{\mu\nu\rho\sigma}\text{Tr}(\hat{F}_{L\mu\nu} + \hat{F}_{R\mu\nu})(\hat{F}_{L\rho\sigma} + \hat{F}_{R\rho\sigma}), \quad (83)$$

where $\epsilon^{0123} = -\epsilon_{0123} = +1$ and,

$$\hat{F}_{L\mu\nu} = \xi^\dagger F_{L\mu\nu} \xi, \quad (84)$$

$$\hat{F}_{R\mu\nu} = \xi F_{R\mu\nu} \xi^\dagger, \quad (85)$$

$$F_{L(R)\mu\nu} = \partial_\mu A_{L(R)\nu} - \partial_\nu A_{L(R)\mu} + i[A_{L(R)\mu}, A_{L(R)\nu}], \quad (86)$$

$$\alpha_{L\mu} = \alpha_\mu + \alpha_{\perp\mu} - gV_\mu, \quad (87)$$

$$\alpha_{R\mu} = \alpha_\mu - \alpha_{\perp\mu} - gV_\mu, \quad (88)$$

$$\alpha_{\perp\mu} = \frac{1}{2i}(\xi^\dagger D_{L\mu} \xi - \xi D_{R\mu} \xi^\dagger). \quad (89)$$

\mathcal{L}_{1-3} given in Eqs.(74-76) are introduced in Refs.[9, 10], while the operator \mathcal{L}_4 is considered in Ref.[12]. Since SU(3) singlet fields are contained in this paper, singlet-induced IPV effect should be taken into account in a way consistent with SU(3) symmetry; \mathcal{L}_{5-10} is written with singlets of η_0 or ϕ_0 . In Eqs.(74-83), the operators are required to be Hermite.

The IP violating parts in R χ PT are denoted as,

$$\mathcal{L}_{\text{IPV}} = \mathcal{L}_{\text{WZ}} + \sum_{i=1}^{10} c_i^{\text{IP}} \mathcal{L}_i. \quad (90)$$

In Eq.(90), the coefficients of the operators, $c_i^{\text{IP}} (i = 1 - 10)$, are free parameters. These parameters should be fixed to fit experimental data so that we focus on the processes which are sensitive to IP violation in this paper. In the following subsections, the analysis of IP violating decay modes is shown for hadronic decays.

In contrast to our work, the singlet fields are contained as a component of chiral nonet matrix in Ref.[12] and $\mathcal{L}_i (i = 5 - 10)$ is not included in that work. Chiral SU(3) breaking effect in IP violating interactions is introduced with spurion field method in Ref.[12], while the operators in Eqs.(74-83) are invariant under SU(3) transformation.

A. Radiative Decays: $V \rightarrow P\gamma$ and $P \rightarrow V\gamma$

In this subsection, IP violating decays of $V \rightarrow P\gamma$ and $P \rightarrow V\gamma$ are investigated. Diagrams contributing to $V \rightarrow P\gamma$ and $P \rightarrow V\gamma$ are listed in Fig.III.1. Interaction vertices of

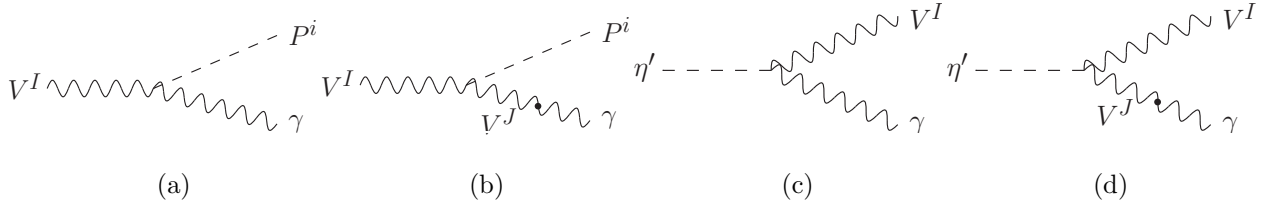


FIG. III.1. Diagrams contributing to the decay width for: (a)-(b) $V^I \rightarrow P^i\gamma$ and (c)-(d) $\eta' \rightarrow V\gamma$.

vector meson are shown in the following as,

$$\mathcal{L}_{\text{IPV}}|_{VP\gamma} = -\frac{e}{f_\pi} \chi_{iI} \epsilon^{\mu\nu\rho\sigma} \partial_\mu V_\nu^I \partial_\rho P^i A_\sigma, \quad (91)$$

$$\mathcal{L}_{\text{IPV}}|_{VVP} = \frac{g}{f_\pi} \theta_{iIJ} \epsilon^{\mu\nu\rho\sigma} \partial_\mu V_\nu^I \partial_\rho P^i V_\sigma^J, \quad (92)$$

$$\begin{aligned} \mathcal{L}_{\text{IPV}}|_{V^+P^-\gamma + \text{h.c.}} &= \frac{2eg}{3f_\pi} c_{34}^- \epsilon^{\mu\nu\rho\sigma} (\partial_\mu \rho_\nu^+ \partial_\rho \pi^- + \partial_\mu \rho_\nu^- \partial_\rho \pi^+) A_\sigma \\ &\quad + \frac{2eg}{3f_K} c_{34}^- \epsilon^{\mu\nu\rho\sigma} (\partial_\mu K_\nu^{*+} \partial_\rho K^- + \partial_\mu K_\nu^{*-} \partial_\rho K^+) A_\sigma \\ &\quad - \frac{4eg}{3f_K} c_{34}^- \epsilon^{\mu\nu\rho\sigma} (\partial_\mu K_\nu^* \partial_\rho \bar{K}^0 + \partial_\mu \bar{K}_\nu^* \partial_\rho K^0) A_\sigma, \end{aligned} \quad (93)$$

$$\begin{aligned} \mathcal{L}_{\text{IPV}}|_{V^-P^+V^0 + \text{h.c.}} &= \frac{g}{f_\pi} \gamma_I \epsilon^{\mu\nu\rho\sigma} (\partial_\mu \rho_\nu^+ \partial_\rho \pi^- + \partial_\mu \rho_\nu^- \partial_\rho \pi^+) V_\sigma^I \\ &\quad + \frac{g}{f_K} L_I \epsilon^{\mu\nu\rho\sigma} (\partial_\mu K_\nu^{*+} \partial_\rho K^- + \partial_\mu K_\nu^{*-} \partial_\rho K^+) V_\sigma^I \\ &\quad - \frac{g}{f_K} \varphi_I \epsilon^{\mu\nu\rho\sigma} (\partial_\mu K_\nu^* \partial_\rho \bar{K}^0 + \partial_\mu \bar{K}_\nu^* \partial_\rho K^0) V_\sigma^I, \end{aligned} \quad (94)$$

where i, I and J run from 1 to 3 and $c_{34}^- = c_3^{\text{IP}} - c_4^{\text{IP}}$. In Eqs.(91-92, 94), fields of mass eigenstate are denoted for vector mesons as $(V^1, V^2, V^3) = (\rho, \omega, \phi)$ and for pseudoscalars as $(P^1, P^2, P^3) = (\pi^0, \eta, \eta')$, respectively. The coefficients, χ_{iI} in Eq.(91), describes the vertex of each component, e.g., χ_{11} for $\rho\pi^0\gamma$ vertex and χ_{12} for $\omega\pi^0\gamma$ vertex. Note that the vertex coefficient of $\rho\omega\pi^0$ is proportional to $\theta_{121} + \theta_{112}$ in Eq.(92) since an operator with $I = 1, J = 2$ and another operator with $I = 2, J = 1$ give the same amplitude. The coefficients of the vertices in Eqs.(91-94) are given as,

$$V^I P^i \gamma : \chi_{iI} = -\frac{2g}{3} c_{34}^- \left[\left(O_{1i} + \sqrt{3} \sqrt{\frac{Z_2^\pi}{Z_1^\pi}} O_{2i} \right) O_{V1I} + \left(\sqrt{3} O_{1i} - \sqrt{\frac{Z_2^\pi}{Z_1^\pi}} O_{2i} \right) O_{V2I} \right] \\ - 4c_5^{\text{IP}} \left(O_{1i} + \frac{1}{\sqrt{3}} \sqrt{\frac{Z_2^\pi}{Z_1^\pi}} O_{2i} \right) O_{V3I} + 2c_8^{\text{IP}} \left(O_{1i} + \frac{1}{\sqrt{3}} \sqrt{\frac{Z_2^\pi}{Z_1^\pi}} O_{2i} \right) O_{V3I} \\ + 2c_9^{\text{IP}} \sqrt{\frac{1}{Z_1^\pi}} O_{3i} \left(O_{V1I} + \frac{1}{\sqrt{3}} O_{V2I} \right), \quad (95)$$

$$V^I V^J P^i : \theta_{iIJ} = -\frac{2gc_3^{\text{IP}}}{\sqrt{3}} \left[\left(2O_{1i} O_{V1I} - \sqrt{\frac{Z_2^\pi}{Z_1^\pi}} O_{2i} O_{V2I} \right) O_{V2J} + \sqrt{\frac{Z_2^\pi}{Z_1^\pi}} O_{2i} O_{V1I} O_{V1J} \right] \\ - 4c_5^{\text{IP}} \left(O_{1i} O_{V3I} O_{V1J} + \sqrt{\frac{Z_2^\pi}{Z_1^\pi}} O_{2i} O_{V3I} O_{V2J} \right) \\ - \frac{2c_6^{\text{IP}}}{g} \sqrt{\frac{1}{Z_1^\pi}} O_{3i} (O_{V1I} O_{V1J} + O_{V2I} O_{V2J}) - \frac{4c_7^{\text{IP}}}{g} \sqrt{\frac{1}{Z_1^\pi}} O_{3i} O_{V3I} O_{V3J}, \quad (96)$$

$$\rho^+ \pi^- V^I + \text{h.c.} : \gamma_I = -\frac{4gc_3^{\text{IP}}}{\sqrt{3}} O_{V2I} - 4c_5^{\text{IP}} O_{V3I}, \quad (97)$$

$$K^{*+} K^- V^I + \text{h.c.} : L_I = -2gc_3^{\text{IP}} \left(O_{V1I} - \frac{1}{\sqrt{3}} O_{V2I} \right) - 4c_5^{\text{IP}} O_{V3I}, \quad (98)$$

$$K^{*0} \bar{K}^0 V^I + \text{h.c.} : \varphi_I = -2gc_3^{\text{IP}} \left(O_{V1I} + \frac{1}{\sqrt{3}} O_{V2I} \right) + 4c_5^{\text{IP}} O_{V3I}. \quad (99)$$

Vector mesons can decay into $P\gamma$ directly with the operator in Eq.(91). $VP\gamma$ vertex is absent in Ref.[12] since the relation $c_3^{\text{IP}} = c_4^{\text{IP}}$ is adopted. Meanwhile, IP violating VVP operator in Eq.(92) also causes $V \rightarrow P\gamma$ with the $V - \gamma$ conversion vertex in Eq.(69). The notation of propagators for neutral vector meson is given as,

$$iD_{\mu\nu}^J(Q) = ig_{\mu\nu} D^J(Q^2) + iQ_\mu Q_\nu D_L^J(Q^2), \quad (J = 1, 2, 3), \quad (100)$$

where $J = 1, 2, 3$ is assigned with the propagator of ρ, ω and ϕ , respectively. In the calculation of the $V - \gamma$ conversion decay $V \rightarrow PV^* \rightarrow P\gamma$, the term proportional to $D_L^J(0)$

vanishes since the momentum product $Q_\mu Q_\nu$ is eliminated when multiplied with antisymmetric tensor. The conversion process $V \rightarrow PV^* \rightarrow P\gamma$ is consequently proportional to the contribution from the metric tensor part of intermediate vector mesons. With Eq.(68), one can find that the following relation are satisfied,

$$D^J(0) \cdot \left(-\frac{e\mathcal{M}_J^2}{g}\eta_J \right) = -\frac{e}{g}\eta_J. \quad (101)$$

Although vector meson propagator reveals apparently in Fig.III.1(b), the dependence on the mass cancels out in Eq.(101). Decay amplitudes are analyzable with the operators in Eqs.(91-94) and written as,

$$\mathcal{M}_{V^I \rightarrow P^i \gamma} = X_{iI} \epsilon^{\mu\nu\rho\sigma} p_\mu^\gamma p_\nu^P \epsilon_\rho^V \epsilon_\sigma^{\gamma*} \quad (102)$$

$$\mathcal{M}_{\rho^+ \rightarrow \pi^+ \gamma} = X_{\rho^+} \epsilon^{\mu\nu\rho\sigma} p_\mu^\gamma p_\nu^{\pi^+} \epsilon_\rho^{\rho^+} \epsilon_\sigma^{\gamma*}, \quad (103)$$

$$\mathcal{M}_{K^{*+} \rightarrow K^+ \gamma} = X_{K^{*+}} \epsilon^{\mu\nu\rho\sigma} p_\mu^\gamma p_\nu^{K^+} \epsilon_\rho^{K^{*+}} \epsilon_\sigma^{\gamma*} \quad (104)$$

$$\mathcal{M}_{K^{*0} \rightarrow K^0 \gamma} = X_{K^{*0}} \epsilon^{\mu\nu\rho\sigma} p_\mu^\gamma p_\nu^{K^0} \epsilon_\rho^{K^{*0}} \epsilon_\sigma^{\gamma*}, \quad (105)$$

$$\mathcal{M}_{\eta' \rightarrow V^I \gamma} = X_{3I} \epsilon^{\mu\nu\rho\sigma} p_\mu^V p_\nu^{\gamma} \epsilon_\rho^{V^*} \epsilon_\sigma^{\gamma*}, \quad (I = 1, 2) \quad (106)$$

$$X_{iI} = \frac{e\sqrt{Z_I}}{f_\pi} \bar{\chi}_{iI}, \quad (107)$$

$$\bar{\chi}_{iI} = \chi_{iI} - \sum_{J=1}^3 \bar{\theta}_{iIJ} \eta_J, \quad (\bar{\theta}_{iIJ} = \theta_{iIJ} + \theta_{iJI}) \quad (108)$$

$$\begin{aligned} &= \frac{2gc_{34}^+}{\sqrt{3}} \left[\left(\sqrt{\frac{Z_2^\pi}{Z_1^\pi}} O_{2i} + \frac{1}{\sqrt{3}} O_{1i} \right) O_{V1I} + \left(O_{1i} - \frac{1}{\sqrt{3}} \sqrt{\frac{Z_2^\pi}{Z_1^\pi}} O_{2i} \right) O_{V2I} \right] \\ &+ \frac{2c_{69}}{g} \sqrt{\frac{1}{Z_1^\pi}} O_{3i} (O_{V1I} + \frac{1}{\sqrt{3}} O_{V2I}) + 2c_8^{\text{IP}} \left(O_{1i} + \frac{1}{\sqrt{3}} \sqrt{\frac{Z_2^\pi}{Z_1^\pi}} O_{2i} \right) O_{V3I}, \end{aligned} \quad (109)$$

$$X_{\rho^+} = \frac{e\sqrt{Z_\rho}}{f_\pi} \left(-\frac{2g}{3} c_{34}^- - \sum_{J=1}^3 \gamma_J \eta_J \right) = \frac{2eg\sqrt{Z_\rho}}{3f_\pi} c_{34}^+, \quad (110)$$

$$X_{K^{*+}} = \frac{e\sqrt{Z_{K^*}}}{f_K} \left(-\frac{2g}{3} c_{34}^- - \sum_{J=1}^3 L_J \eta_J \right) = \frac{2eg\sqrt{Z_{K^*}}}{3f_K} c_{34}^+, \quad (111)$$

$$X_{K^{*0}} = \frac{e\sqrt{Z_{K^*}}}{f_K} \left(\frac{4g}{3} c_{34}^- + \sum_{J=1}^3 \varphi_J \eta_J \right) = -\frac{4eg\sqrt{Z_{K^*}}}{3f_K} c_{34}^+, \quad (112)$$

where $c_{34}^+ = c_3^{\text{IP}} + c_4^{\text{IP}}$ and $c_{69} = 2c_6^{\text{IP}} + gc_9^{\text{IP}}$. The coefficient of neutral meson decay amplitude denoted as X_{iI} in Eq.(107) includes the factor $(\sqrt{Z_1}, \sqrt{Z_2}, \sqrt{Z_3}) = (\sqrt{Z_\rho}, \sqrt{Z_\omega}, \sqrt{Z_\phi})$ which comes from the wave function renormalization of an external vector line in Fig.III.1. In Eqs.(110, 111), we assume that the wave function renormalization of charged vector meson

is equal to one for neutral vector meson, i.e., $\sqrt{Z_{\rho^+}} = \sqrt{Z_{\rho}}$ and $\sqrt{Z_{K^*}} = \sqrt{Z_{K^{*+}}}$ which is valid in the isospin limit. One can write the partial decay width of $V \rightarrow P\gamma$ and $P \rightarrow V\gamma$ with X 's in Eqs.(107, 110-112) as,

$$\Gamma[V^I \rightarrow P^i\gamma] = \frac{1}{96\pi} X_{iI}^2 m_I^3 \left(1 - \frac{M_{P^i}^2}{m_I^2}\right)^3, \quad (113)$$

$$\Gamma[\rho^+ \rightarrow \pi^+\gamma] = \frac{1}{96\pi} X_{\rho^+}^2 m_{\rho^+}^3 \left(1 - \frac{M_{\pi^+}^2}{m_{\rho^+}^2}\right)^3, \quad (114)$$

$$\Gamma[K^{*+} \rightarrow K^+\gamma] = \frac{1}{96\pi} X_{K^{*+}}^2 m_{K^{*+}}^3 \left(1 - \frac{M_{K^+}^2}{m_{K^{*+}}^2}\right)^3, \quad (115)$$

$$\Gamma[K^{*0} \rightarrow K^0\gamma] = \frac{1}{96\pi} X_{K^{*0}}^2 m_{K^{*0}}^3 \left(1 - \frac{M_{K^0}^2}{m_{K^{*0}}^2}\right)^3, \quad (116)$$

$$\Gamma[\eta' \rightarrow V^I\gamma] = \frac{1}{32\pi} X_{3I}^2 M_{\eta'}^3 \left(1 - \frac{m_I^2}{M_{\eta'}^2}\right)^3. \quad (I = 1, 2) \quad (117)$$

The pseudoscalar decay width in Eq.(117) is analogous to one for $V \rightarrow P\gamma$ given in Eqs.(113-116) and its coefficient is different by a factor 1/3 which comes from spin average of vector meson. Note that the widths in Eqs.(113-117) include the parameters c_{34}^+ , c_{69} and c_8^{IP} so that we constrain them via experimental data. One can find that $\Gamma_{V^I \rightarrow P^i\gamma}$ and $\Gamma_{\rho^+ \rightarrow \pi^+\gamma}$ in Eqs.(113-114) provide the relation as,

$$\left| \frac{X_{iI}}{X_{\rho^+}} \right| = \sqrt{\frac{\Gamma_{V^I \rightarrow P^i\gamma}}{\Gamma_{\rho^+ \rightarrow \pi^+\gamma}} \frac{m_I^3}{m_{\rho^+}^3} \left(\frac{m_{\rho^+}^2 - M_{\pi^+}^2}{m_I^2 - M_{P^i}^2} \right)^3}. \quad (118)$$

Hence, the ratio of the effective couplings for $V^I \rightarrow P^i\gamma$ to $\rho^+ \rightarrow \pi^+\gamma$ are described by the experimental data on r.h.s. in Eq.(118). Plugging Eqs.(113-114) into Eq.(118), one obtains,

$$\begin{aligned} & \sqrt{\frac{Z_I}{Z_{\rho^+}}} \left| O_{1i}(O_{V1I} + \sqrt{3}O_{V2I}) + \sqrt{\frac{Z_2^\pi}{Z_1^\pi}} O_{2i}(\sqrt{3}O_{V1I} - O_{V2I}) \right. \\ & \left. + \frac{\sqrt{3}c_{69}}{g^2 c_{34}^+} \sqrt{\frac{1}{Z_1^\pi}} O_{3i}(\sqrt{3}O_{V1I} + O_{V2I}) + \frac{\sqrt{3}c_8^{\text{IP}}}{g c_{34}^+} \left(\sqrt{3}O_{1i} + \sqrt{\frac{Z_2^\pi}{Z_1^\pi}} O_{2i} \right) O_{V3I} \right| \\ & = \sqrt{\frac{\Gamma_{V^I \rightarrow P^i\gamma}}{\Gamma_{\rho^+ \rightarrow \pi^+\gamma}} \frac{m_I^3}{m_{\rho^+}^3} \left(\frac{m_{\rho^+}^2 - M_{\pi^+}^2}{m_I^2 - M_{P^i}^2} \right)^3}. \end{aligned} \quad (119)$$

where in the above equation, l.h.s is expressed in terms of the parameters. We use the relation in Eq.(119) for the numerical analysis of χ^2 fitting.

B. $\phi \rightarrow \omega \pi^0$

In this subsection, an IP violating process of $\phi \rightarrow \omega \pi^0$ is analyzed. The contributing operator to $\phi \rightarrow \omega \pi^0$ is given in Eq.(92), and the diagram is shown in Fig.III.2. The

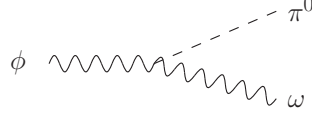


FIG. III.2. Diagrams contributing to the IP violating decay of $\phi \rightarrow \omega \pi^0$.

transition amplitude of $\phi \rightarrow \omega \pi^0$ is written as,

$$\mathcal{M}_{\phi \rightarrow \omega \pi^0} = X_{\phi \rightarrow \omega \pi^0} \epsilon^{\mu\nu\rho\sigma} p_\mu^\omega p_\nu^{\pi^0} \epsilon_\rho^\phi \epsilon_\sigma^{\omega*}, \quad (120)$$

$$X_{\phi \rightarrow \omega \pi^0} = -\frac{g\sqrt{Z_\phi Z_\omega}}{f_\pi} \bar{\theta}_{123}. \quad (121)$$

The contribution coming from $V - \gamma$ conversion is negligible since it gives rise to $\mathcal{O}(\alpha)$ correction. In Eq.(121), the factor of wave function renormalization of external vectors is included. Thus, the partial decay width of $\phi \rightarrow \omega \pi^0$ is,

$$\Gamma[\phi \rightarrow \omega \pi^0] = \frac{1}{96\pi} X_{\phi \rightarrow \omega \pi^0}^2 \times \left(\frac{\sqrt{m_\phi^4 + m_\omega^4 + M_{\pi^0}^4 - 2(m_\phi^2 m_\omega^2 + m_\omega^2 M_{\pi^0}^2 + M_{\pi^0}^2 m_\phi^2)}}{m_\phi} \right)^3. \quad (122)$$

C. $P \rightarrow 2\gamma$

In this subsection, we evaluate partial decay widths of the IP violating process given as $P^i \rightarrow 2\gamma$. The IP violating interaction terms yield contribution to $P\gamma\gamma$ vertex as,

$$\mathcal{L}_{\text{IPV}}|_{P^i\gamma\gamma} = -\frac{e^2}{f_\pi} h_i \epsilon^{\mu\nu\rho\sigma} P^i \partial_\mu A_\nu \partial_\rho A_\sigma, \quad (123)$$

$$h_i = \left(\frac{1}{8\pi^2} + \frac{4c_4^{\text{IP}}}{3} \right) \left(O_{1i} + \frac{1}{\sqrt{3}} \sqrt{\frac{Z_2^\pi}{Z_1^\pi}} O_{2i} \right) - \frac{32}{3} c_{10}^{\text{IP}} \sqrt{\frac{1}{Z_1^\pi}} O_{3i}, \quad (124)$$

where the first term proportional to $1/8\pi^2$ in Eq.(124) implies the contribution from the WZW term. Diagrams of the decay of $P^i \rightarrow 2\gamma$ are given in Fig.III.3. With the operators

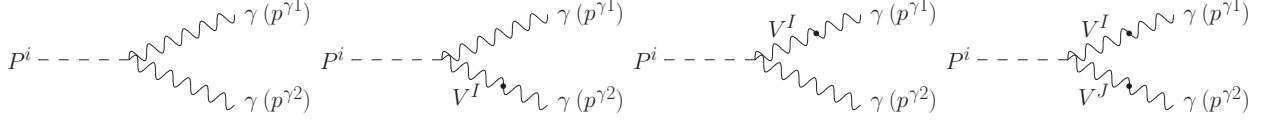


FIG. III.3. Diagrams contributing to the decay width of $P^i \rightarrow 2\gamma$.

in Eqs.(69, 91, 123), the transition amplitude of $P^i \rightarrow 2\gamma$ is written as,

$$\mathcal{M}_{P^i \rightarrow 2\gamma} = R_i \epsilon^{\mu\nu\rho\sigma} p_\mu^{\gamma 1} p_\nu^{\gamma 2} \epsilon_\rho^{\gamma 1*} \epsilon_\sigma^{\gamma 2*}, \quad (125)$$

$$\begin{aligned} R_i &= -\frac{e^2}{f_\pi} \left[2h_i - \frac{1}{g} \left(2 \sum_{I=1}^3 \chi_{iI} \eta_I - \sum_{I,J=1}^3 \bar{\theta}_{iIJ} \eta_I \eta_J \right) \right] \\ &= -\frac{e^2}{f_\pi} \left[\frac{1}{4\pi^2} \left(O_{1i} + \frac{1}{\sqrt{3}} \sqrt{\frac{Z_2^\pi}{Z_1^\pi}} O_{2i} \right) - \frac{16}{3} c_{6-9-10} \sqrt{\frac{1}{Z_1^\pi}} O_{3i} \right]. \end{aligned} \quad (126)$$

where $c_{6-9-10} = c_6^{\text{IP}}/g^2 + c_9^{\text{IP}} + 4c_{10}^{\text{IP}}$. Hence one can find that the partial decay width of $P^i \rightarrow 2\gamma$ is given as,

$$\Gamma[P^i \rightarrow 2\gamma] = \frac{1}{64\pi} R_i^2 M_{P^i}^3. \quad (127)$$

D. $P \rightarrow \gamma l^+ l^-$

In this subsection, a form factor for IP violating modes $P^i \rightarrow \gamma l^+ l^-$ is obtained. The contributing diagrams are displayed in Fig.III.4. Following the notations used in experiments,

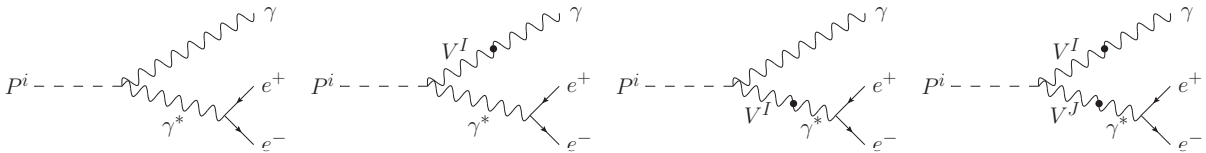


FIG. III.4. Diagrams contributing to the decay width of $P^i \rightarrow \gamma l^+ l^-$.

the differential decay width is written in terms of the TFF as,

$$\frac{d\Gamma(P^i \rightarrow \gamma l^+ l^-)}{ds d\cos\theta} = \frac{\alpha}{4\pi} \Gamma(P^i \rightarrow 2\gamma) \frac{\beta_l}{s} (2 - \beta_l^2 \sin^2\theta) \left(1 - \frac{s}{M_{P^i}^2} \right)^3 |F_{P^i}(s)|^2, \quad (128)$$

$$\frac{d\Gamma(P^i \rightarrow \gamma l^+ l^-)}{ds} = \frac{2\alpha}{3\pi} \Gamma(P^i \rightarrow 2\gamma) \frac{\beta_l}{s} \left(1 + \frac{2m_l^2}{s} \right) \left(1 - \frac{s}{M_{P^i}^2} \right)^3 |F_{P^i}(s)|^2, \quad (129)$$

where $\beta_l = \sqrt{1 - 4m_l^2/s}$, s denotes the squared invariant mass in di-lepton system and θ indicates an angle between P^i and l^+ in the di-lepton rest frame. The model prediction for

the TFF is determined with,

$$|F_{P^i}(s)|^2 = \left| 1 + \frac{e^2 s}{g f_\pi R_i} \sum_{I=1}^3 \bar{\chi}_{iI} \eta_I \delta B_{VI} D_I(s) \right|^2. \quad (130)$$

E. $V \rightarrow Pl^+l^-$

In this subsection, a form factor for IP violating electromagnetic decays for neutral vector mesons are analyzed. Tree level diagrams are exhibited in Fig.III.5. The partial decay width

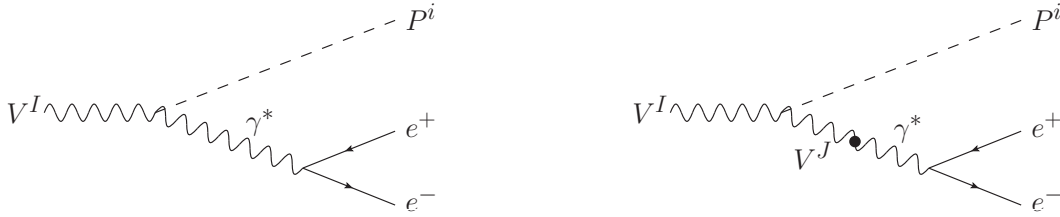


FIG. III.5. Diagrams contributing to the decay width of $V^I \rightarrow P^i l^+ l^-$.

is defined with a TFF as,

$$\frac{d^2\Gamma(V^I \rightarrow P^i l^+ l^-)}{ds d\cos\theta} = \frac{\alpha}{8\pi} \Gamma(V^I \rightarrow P^i \gamma) \frac{\beta_l}{s} (2 - \beta_l^2 \sin^2\theta) \times \left[\left(1 + \frac{s}{m_I^2 - M_{P^i}^2} \right)^2 - \frac{4m_I^2 s}{(m_I^2 - M_{P^i}^2)^2} \right]^{\frac{3}{2}} |F_{V^I P^i}(s)|^2, \quad (131)$$

$$\frac{d\Gamma(V^I \rightarrow P^i l^+ l^-)}{ds} = \frac{\alpha}{3\pi} \Gamma(V^I \rightarrow P^i \gamma) \frac{\beta_l}{s} \left(1 + \frac{2m_l^2}{s} \right) \times \left[\left(1 + \frac{s}{m_I^2 - M_{P^i}^2} \right)^2 - \frac{4m_I^2 s}{(m_I^2 - M_{P^i}^2)^2} \right]^{\frac{3}{2}} |F_{V^I P^i}(s)|^2, \quad (132)$$

where θ is an angle between V^I and l^+ in the di-lepton rest frame. The TFF as the model prediction is formulated with,

$$|F_{V^I P^i}(s)|^2 = \left| 1 + \frac{s}{\bar{\chi}_{iI}} \sum_{J=1}^3 \bar{\theta}_{iIJ} \eta_J \delta B_{VJJ} D_J(s) \right|^2. \quad (133)$$

The TFF in the above equation are normalized to be unity in the limit where virtual photon goes on shell.

F. $V \rightarrow P\pi^+\pi^-$

In this subsection, partial decay widths for $V \rightarrow P\pi^+\pi^-$ are analyzed. Interaction terms for the process are,

$$\mathcal{L}_{\text{IPV}}|_{V^I P^i \pi^+ \pi^-} = i \frac{J_{iI}}{f_\pi^3} \epsilon^{\mu\nu\rho\sigma} V_\mu^I \partial_\nu P^i \partial_\rho \pi^+ \partial_\sigma \pi^-, \quad (134)$$

$$\mathcal{L}_\chi|_{\rho^- P^i \pi^+ + \text{h.c.}} = i g_{\rho\pi\pi} O_{1i} \left[\rho_\mu^- \left(P^i \overleftrightarrow{\partial}^\mu \pi^+ \right) - \rho_\mu^+ \left(P^i \overleftrightarrow{\partial}^\mu \pi^- \right) \right], \quad (135)$$

$$J_{iI} = \frac{g c_{123}}{\sqrt{3}} \left(3 O_{1i} O_{V2I} + \sqrt{\frac{Z_2^\pi}{Z_1^\pi}} O_{2i} O_{V1I} \right) + 12 c_5^{\text{IP}} O_{1i} O_{V3I}, \quad (136)$$

where Π_I is defined in Eq.(49) and $c_{123} = c_{12}^- + 2c_3^{\text{IP}}$. The diagrams of the decay of $V^I \rightarrow P^i \pi^+ \pi^-$ are given in Fig.III.6. Propagators for ρ^\pm are formulated in the following form as,

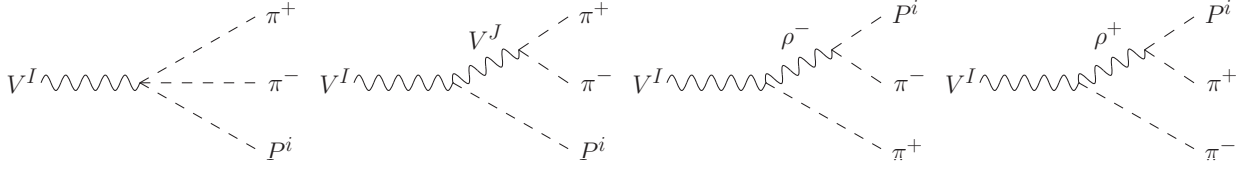


FIG. III.6. Diagrams contributing to the decay width of $V^I \rightarrow P^i \pi^+ \pi^-$.

$$i D_\pm^{\mu\nu}(Q) = i g^{\mu\nu} D_\pm(Q^2) + i Q^\mu Q^\nu D_{L\pm}(Q^2). \quad (137)$$

The transition amplitude is given as,

$$\mathcal{M} = Y_{iI} \epsilon^{\mu\nu\rho\sigma} \epsilon_\mu^V p_\nu^- p_\rho^+ p_\sigma^0, \quad (138)$$

$$Y_{iI} = \frac{\sqrt{Z_I}}{f_\pi^3} \left[J_{iI} + \sum_{J=1}^3 \zeta_{iIJ} D^J(s_{+-}) + \kappa_{iI} (D_+(s_{+0}) + D_-(s_{-0})) \right], \quad (139)$$

$$\zeta_{iIJ} = 2M_V^2 \bar{\theta}_{iIJ} \Pi_J, \quad \kappa_{iI} = M_V^2 O_{1i} \gamma_I, \quad (140)$$

where s_{+0}, s_{-0} and s_{+-} are squared invariant masses for the $\pi^+ P^i, \pi^- P^i$ and $\pi^+ \pi^-$ system, respectively. s_{+-} is kinematically related with the other variables as $s_{+-} = m_I^2 + 2M_{\pi^+}^2 + M_{P^i}^2 - s_{+0} - s_{-0}$. The formula of the partial decay width is obtained as,

$$\Gamma[V^I \rightarrow P^i \pi^+ \pi^-] = \frac{1}{3072 \pi^3 m_I^3} \iint_{(M_{\pi^+} + M_{P^i})^2}^{(m_I - M_{\pi^+})^2} |Y_{iI}|^2 H \theta(H) ds_{+0} ds_{-0}, \quad (141)$$

$$H = s_{+-} [s_{+0} s_{-0} + (m_I^2 - M_{\pi^+}^2)(M_{\pi^+}^2 - M_{P^i}^2)] - M_{\pi^+}^2 (m_I^2 - M_{P^i}^2)^2, \quad (142)$$

where in the above equation $\theta(H)$ denotes step function, and the integral regions are common for s_{+0} and s_{-0} .

G. $P \rightarrow \pi^+ \pi^- \gamma$

In this subsection, differential decay widths for $P \rightarrow \pi^+ \pi^- \gamma$ are calculated. The diagrams contributing to this process are given in Fig.III.7. The transition amplitude for the process

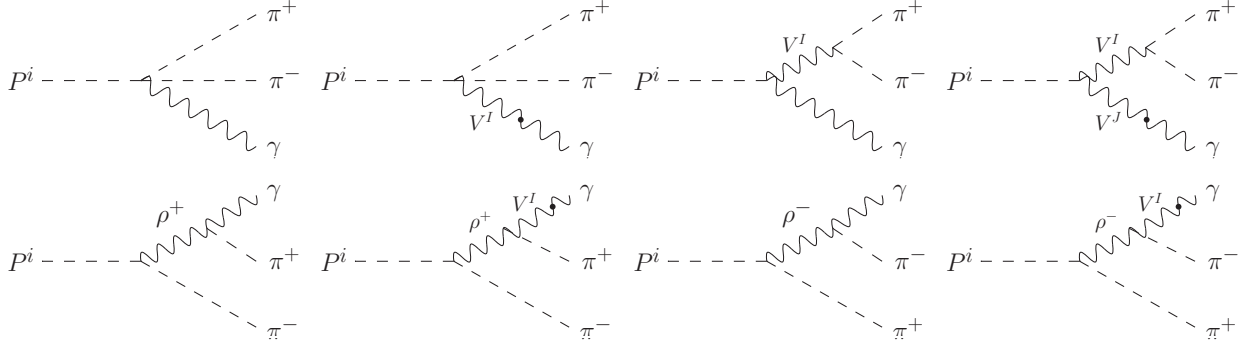


FIG. III.7. Diagrams contributing to the decay width for $P^i \rightarrow \pi^+ \pi^- \gamma$.

$P^i \rightarrow \pi^+ \pi^- \gamma (i = 2, 3)$ is,

$$\mathcal{M}_{P^i \rightarrow \pi^+ \pi^- \gamma} = Y_i^\gamma \epsilon^{\mu\nu\rho\sigma} \epsilon_\mu^{\gamma*} p_\nu^- p_\rho^+ p_\sigma^\gamma, \quad (143)$$

$$Y_i^\gamma = -\frac{e}{f_\pi^3} [\bar{A}_i + \bar{B}_{iI} D^I(s) + \bar{C}_i (D_+(s_{+0}) + D_-(s_{-0}))], \quad (144)$$

$$\begin{aligned} \bar{A}_i &= \left(\frac{1}{4\pi^2} + 2c_{34}^+ \right) \left(O_{1i} + \frac{1}{\sqrt{3}} \sqrt{\frac{Z_2^\pi}{Z_1^\pi}} O_{2i} \right), \\ \bar{B}_{iI} &= -4g_{\rho\pi\pi} f_\pi^2 \bar{\chi}_{iI} \Pi^I, \quad \bar{C}_i = -\frac{4g_{\rho\pi\pi} f_\pi^2}{3} g c_{34}^+ O_{1i}. \end{aligned} \quad (145)$$

Hence, the differential decay width is given as,

$$\frac{d^2\Gamma[P^i \rightarrow \pi^+ \pi^- \gamma]}{ds d\cos\theta} = \frac{1}{8192\pi^3 M_{P^i}^3} |Y_i^\gamma|^2 \sin^2\theta s^4 \beta_{\pi^+}^3 \left(1 - \frac{M_{P^i}^2}{s} \right)^3, \quad (146)$$

where s denotes the squared invariant mass in $\pi^+ \pi^-$ system and θ implies the angle between π^+ and γ in the rest frame of $\pi^+ \pi^-$.

IV. NUMERICAL ANALYSIS

In this section, phenomenological analysis is carried out in the $R\chi PT$ model. We perform χ^2 fitting for experimental data of the decay widths of hadrons and masses of ρ, ω and ϕ to obtain the model parameters in the following subsection. The di-lepton mass distributions of the Dalitz decays are also fitted so that one can obtain the parameter range of the coefficients

of the IP violating operators. Subsequently, the prediction of the model is presented for Dalitz distributions and partial decay widths of IP violating modes.

A. Parameter fit

1. Mass and width of vector mesons

In this subsection, we fix the parameters, $g_{\rho\pi\pi}$, C_1^r , Z_V^r , \hat{g}_{1V} and M_{0V} , and evaluate the vector meson mass, the renormalization constant and the decay width.

At first, we consider the off-diagonal elements of V_μ , i.e., ρ^+ , K^{*+} and K^{*0} to obtain the parameters, $g_{\rho\pi\pi}$, C_1^r and Z_V^r . We define the masses of ρ^+ and K^{*+} mesons as the momentum-squared for which real parts of inverse propagators vanish,

$$M_V^2 + \text{Re}[\delta A_{\rho^+}(Q^2 = m_{\rho^+}^2; C_1^r, C_2^r)] = 0, \quad (147)$$

$$M_V^2 + \text{Re}[\delta A_{K^{*+}}(Q^2 = m_{K^{*+}}^2; C_1^r, C_2^r)] = 0, \quad (148)$$

where δA_{ρ^+} and $\delta A_{K^{*+}}$ are shown in Eqs. (C15) and (C19), respectively. Solving the above equations, we have C_1^r and C_2^r ,

$$C_1^r = \frac{1}{\Delta_{K^+\pi}} \{ Z_V^r \Delta_{K^{*+}\rho^+} - \text{Re}[\Delta A_{K^{*+}}(m_{K^{*+}}^2)] + \text{Re}[\Delta A_{\rho^+}(m_{\rho^+}^2)] \}, \quad (149)$$

$$C_2^r = -\frac{1}{2\bar{M}_K^2 + M_\pi^2} \{ M_V^2 - Z_V^r m_{K^{*+}}^2 + \text{Re}[\Delta A_{K^{*+}}(m_{K^{*+}}^2)] + C_1^r M_{K^+}^2 \}. \quad (150)$$

Imposing the condition for the residue of the vector meson propagator, $\text{Res}D(Q^2 = m_{K^{*+}}^2) = 1$, we have

$$Z_V^r = 1 + \left. \frac{d\text{Re}[\Delta A_{K^{*+}}(Q^2)]}{dQ^2} \right|_{Q^2=m_{K^{*+}}^2}. \quad (151)$$

Since ΔA_V only depends on $g_{\rho\pi\pi}$, C_1^r and Z_V^r can be fixed by $g_{\rho\pi\pi}$. On the other hand, C_2^r is related to two parameters, $g_{\rho\pi\pi}$ and M_V .

To fix the value of $g_{\rho\pi\pi}$, we use the decay widths for $\rho \rightarrow \pi\pi$, $K^{*\pm} \rightarrow (K\pi)^\pm$ and $K^{*0} \rightarrow (K\pi)^0$. The decay widths are given by the imaginary part of the inverse propagators,

$$m_I \Gamma_I = -Z_I \text{Im}[\delta A_I(m_I^2)], \quad (152)$$

where $I = \rho^+, K^{*+}, K^{*0}$,

$$(Z_I)^{-1} = Z_V^r - \left. \frac{d\text{Re}[\Delta A_I(Q^2)]}{dQ^2} \right|_{Q^2=m_I^2}, \quad (153)$$

where ΔA_I is defined in Eqs.(C16, C18, C20). $g_{\rho\pi\pi}$ is fixed to realize the minimum of χ^2 of the decay widths for $V^I \rightarrow PP$. The fitted results of the widths are shown in Table I. The

TABLE I. The results of the decay widths for $V \rightarrow PP$.

Decay mode	Theory (MeV)	PDG (MeV)
$\Gamma[\rho \rightarrow \pi\pi]$	152.0 ± 0.7	149.1 ± 0.8
$\Gamma[K^{*\pm} \rightarrow (K\pi)^\pm]$	42.5 ± 0.2	46.2 ± 1.3
$\Gamma[K^{*0} \rightarrow (K\pi)^0]$	42.2 ± 0.2	47.4 ± 0.6

parameters C_1^r and Z_V^r , and the renormalization constants Z_i are estimated as follows,

$$\begin{aligned}
g_{\rho\pi\pi} &= 5.83 \pm 0.01, \quad C_1^r = 0.373 \pm 0.002, \quad Z_V^r = 0.8457 \pm 0.0007, \\
Z_{\rho^+} &= 1.0389 \pm 0.0002, \quad Z_{K^{*0}} = 1.00207 \pm 0.00001.
\end{aligned}
\tag{154}$$

Next, we determine the parameters \hat{g}_{1V} and M_{0V} with the χ^2 fitting of the neutral vector meson mass in Eq.(44). The fitted results of the neutral vector meson mass are shown in Table II, where the obtained $\chi^2/\text{n.d.f}$ is 6.72/1. The parameters \hat{g}_{1V} and M_{0V} are fixed as,

$$\hat{g}_{1V} = 3.20, \quad M_{0V} = 875.5\text{MeV}.
\tag{155}$$

Using the above parameters, we have the orthogonal matrix O_V which diagonalizes vector

TABLE II. The results of the neutral vector meson mass.

Mass	Theory(MeV)	PDG (MeV)
m_{ρ^0}	774.61	775.26 ± 0.25
m_ω	782.65	782.65 ± 0.12
m_ϕ	1019.46	1019.461 ± 0.019

meson mass matrix,

$$O_V = \begin{pmatrix} 0.996 & 0.0861 & -0.00333 \\ -0.0586 & 0.649 & -0.759 \\ -0.0631 & 0.756 & 0.652 \end{pmatrix},
\tag{156}$$

where $\omega - \phi$ mixing angle is 40.7° . The wave function renormalization of the neutral vector meson and the eigenvalues for the mass matrix are obtained as follows,

$$\begin{aligned} Z_{\rho^0} &= 1.039, & Z_\omega &= 1.024, & Z_\phi &= 0.929, \\ \mathcal{M}_1 &= 789.3\text{MeV}, & \mathcal{M}_2 &= 766.1\text{MeV}, & \mathcal{M}_3 &= 1005\text{MeV}. \end{aligned} \quad (157)$$

2. Intrinsic parity violating decays

To estimate values of the IP violating parameters, experimental data of branching ratios and Dalitz distributions are used for the χ^2 fitting. In the procedure of fitting, one can determine fourteen free parameters in the model. As experimental data, we adopt the data of PDG[23] for IP violating partial decay widths of vector meson. In Table III, the partial decay widths are exhibited with $|gc_{34}^+| = 0.107 \pm 0.04$, which realizes the minimum of χ^2 . As theoretical values, the result of the R χ PT model is shown and compared with PDG values.

TABLE III. Partial decay widths of charged vector meson as χ^2 fitting result.

Decay mode	Theory (MeV)	PDG (MeV)
$\Gamma[\rho^+ \rightarrow \pi^+\gamma]$	$(8.0 \pm 0.6) \times 10^{-2}$	$(6.7 \pm 0.7) \times 10^{-2}$
$\Gamma[K^{*+} \rightarrow K^+\gamma]$	$(3.1 \pm 0.2) \times 10^{-2}$	$(5.0 \pm 0.5) \times 10^{-2}$
$\Gamma[K^{*0} \rightarrow K^0\gamma]$	0.121 ± 0.009	0.12 ± 0.01

Since the mass matrix of pseudoscalars includes many undetermined parameters, it is difficult to fix the mixing angles which diagonalize 1-loop corrected mass matrix in Eq.(F10). To determine the mixing angles, we conduct χ^2 fitting with respect to the experimental data of the widths for $P^i \rightarrow 2\gamma, \eta' \rightarrow \omega\gamma$ and the ratio of effective coupling of $V^I P^i \gamma$ to one for $\rho^+ \pi^+ \gamma$ and f_{K^-}/f_{π^-} . The minimum of χ^2 is realized with the parameters,

$$\begin{aligned} g &= 4.80, & L_4^r &= 7.4 \times 10^{-4}, & L_5^r &= 3.0 \times 10^{-3}, & c_{6-9-10} &= 7.5 \times 10^{-3}, \\ \frac{c_{69}}{g^2} \frac{1}{c_{34}^+} &= -0.50, & \frac{c_8^{\text{IP}}}{gc_{34}^+} &= 0.78, & \theta_1 &= 0.36, & \theta_2 &= 5.5 \times 10^{-2}, & \theta_3 &= 5.6 \times 10^{-2}, \end{aligned} \quad (158)$$

where $\eta - \eta'$ mixing angle is determined to be 20.9° . We found that the mixing matrix O determined by the fitting does not exactly diagonalize the 1-loop corrected mass matrix in Eq.(F10). For further consistency, one should take account of diagonalization of the mass matrix. The widths and f_{K^-}/f_{π^-} as theoretical values are exhibited in Table IV, and

effective coupling ratio $|X_{iI}/X_{\rho^+}|$ are shown in Table V. Here, we discuss a case that singlet-induced contribution is absent. If one takes the limit $c_{6-9-10} \rightarrow 0$, the partial width of η' becomes $\Gamma[\eta' \rightarrow 2\gamma] = 0.08 \times 10^{-3} \text{MeV}$. This value is much smaller than the experimental data. Hence, one notices that the presence of singlet-induced IP violation is necessary in the framework of singlet+octet scheme.

TABLE IV. Partial decay widths of IP violating mode and the ratio of decay constant for K^- to one for π^- . For comparison, PDG data[23] are also exhibited.

	Theory (MeV)	PDG (MeV)
$\Gamma[\pi^0 \rightarrow 2\gamma]$	7.6×10^{-6}	$(7.6 \pm 0.2) \times 10^{-6}$
$\Gamma[\eta \rightarrow 2\gamma]$	5.2×10^{-4}	$(5.2 \pm 0.2) \times 10^{-4}$
$\Gamma[\eta' \rightarrow 2\gamma]$	4.5×10^{-3}	$(4.4 \pm 0.2) \times 10^{-3}$
$\Gamma[\rho^0 \rightarrow \pi^0 \gamma]$	4.3×10^{-2}	$(8.9 \pm 1.2) \times 10^{-2}$
$\Gamma[\omega \rightarrow \pi^0 \gamma]$	0.73	0.70 ± 0.03
$\Gamma[\phi \rightarrow \pi^0 \gamma]$	7.1×10^{-3}	$(5.4 \pm 0.3) \times 10^{-3}$
$\Gamma[\rho \rightarrow \eta \gamma]$	3.5×10^{-2}	$(4.4 \pm 0.3) \times 10^{-2}$
$\Gamma[\omega \rightarrow \eta \gamma]$	5.3×10^{-3}	$(3.9 \pm 0.3) \times 10^{-3}$
$\Gamma[\phi \rightarrow \eta \gamma]$	1.2×10^{-2}	$(5.5 \pm 0.1) \times 10^{-2}$
$\Gamma[\phi \rightarrow \eta' \gamma]$	3.4×10^{-4}	$(2.67 \pm 0.09) \times 10^{-4}$
$\Gamma[\eta' \rightarrow \omega \gamma]$	4.1×10^{-3}	$(5.4 \pm 0.5) \times 10^{-3}$
f_{K^-}/f_{π^-}	1.172	1.197 ± 0.009

In the following, Dalitz decays of $V^I \rightarrow P^i l^+ l^-$ are analyzed. The IP violating parameters, $c_i^{\text{IP}} (i = 3-10)$, are determined to realize the minimum of χ^2 . We fit the experimental data of form factors, $|F_{V^I P^i}|^2$, in each bin for di-lepton invariant mass. The obtained distributions, which result from $\chi_0^2/\text{d.o.f.} = 190.6/151$, are exhibited in Fig.IV.1. Using the obtained value of M_V , we have C_2^r in Eq. (150) as $C_2^r = 0.0913$ and the decay widths for $V^I \rightarrow PP$ in Eq.(51). The result of the decay widths are seen in Table VI. The parameters fixed in this subsection are shown in Table VII.

TABLE V. Values of $|X_{iI}/X_{\rho^+}|$: the ratio of effective coupling in $V^I \rightarrow P^i \gamma$ to one for $\rho^+ \rightarrow \pi^+ \gamma$. For comparison, the experimental data extracted from PDG data[23] are also exhibited. In the rightest column, the model prediction in the isospin limit is displayed with wave function renormalizations set as unity. The mixing angle of vector meson denotes $\cos \theta_V^{08} = O_{V22} \sim O_{V33}$ and $\sin \theta_V^{08} = O_{V23} \sim -O_{V32}$.

Ratio	PDG	Theory	Model in the isospin limit
$\frac{X_{11}}{X_{\rho^+}}$	1.15 ± 0.10	0.73	1
$\frac{X_{12}}{X_{\rho^+}}$	3.2 ± 0.2	3.0	$\sqrt{3} \cos \theta_V^{08} - \frac{3c_8^{\text{IP}}}{gc_{34}^+} \sin \theta_V^{08} $
$\frac{X_{13}}{X_{\rho^+}}$	0.18 ± 0.01	0.19	$\sqrt{3} \sin \theta_V^{08} + \frac{3c_8^{\text{IP}}}{gc_{34}^+} \cos \theta_V^{08} $
$\frac{X_{21}}{X_{\rho^+}}$	2.2 ± 0.1	1.8	$\sqrt{3} \cos \theta_1 - (\frac{c_{69}}{g^2 c_{34}}) \tan \theta_1 $
$\frac{X_{22}}{X_{\rho^+}}$	0.62 ± 0.05	0.66	$ \cos \theta_V^{08} \cos \theta_1 + \sqrt{3} (\frac{c_{69}}{g^2 c_{34}}) \sin \theta_1 - \frac{\sqrt{3} c_8^{\text{IP}}}{gc_{34}^+} \cos \theta_1 \tan \theta_V^{08} $
$\frac{X_{23}}{X_{\rho^+}}$	0.96 ± 0.06	0.41	$ \sin \theta_V^{08} \cos \theta_1 + \sqrt{3} (\frac{c_{69}}{g^2 c_{34}}) \sin \theta_1 + \frac{\sqrt{3} c_8^{\text{IP}}}{gc_{34}^+} \cos \theta_1 \cot \theta_V^{08} $
$\frac{X_{33}}{X_{\rho^+}}$	0.99 ± 0.06	1.02	$ \sin \theta_V^{08} \sin \theta_1 - \sqrt{3} (\frac{c_{69}}{g^2 c_{34}}) \cos \theta_1 + \frac{\sqrt{3} c_8^{\text{IP}}}{gc_{34}^+} \sin \theta_1 \cot \theta_V^{08} $
$\frac{X_{32}}{X_{\rho^+}}$	0.59 ± 0.04	0.47	$ \cos \theta_V^{08} \sin \theta_1 - \sqrt{3} (\frac{c_{69}}{g^2 c_{34}}) \cos \theta_1 - \frac{\sqrt{3} c_8^{\text{IP}}}{gc_{34}^+} \sin \theta_1 \cot \theta_V^{08} $

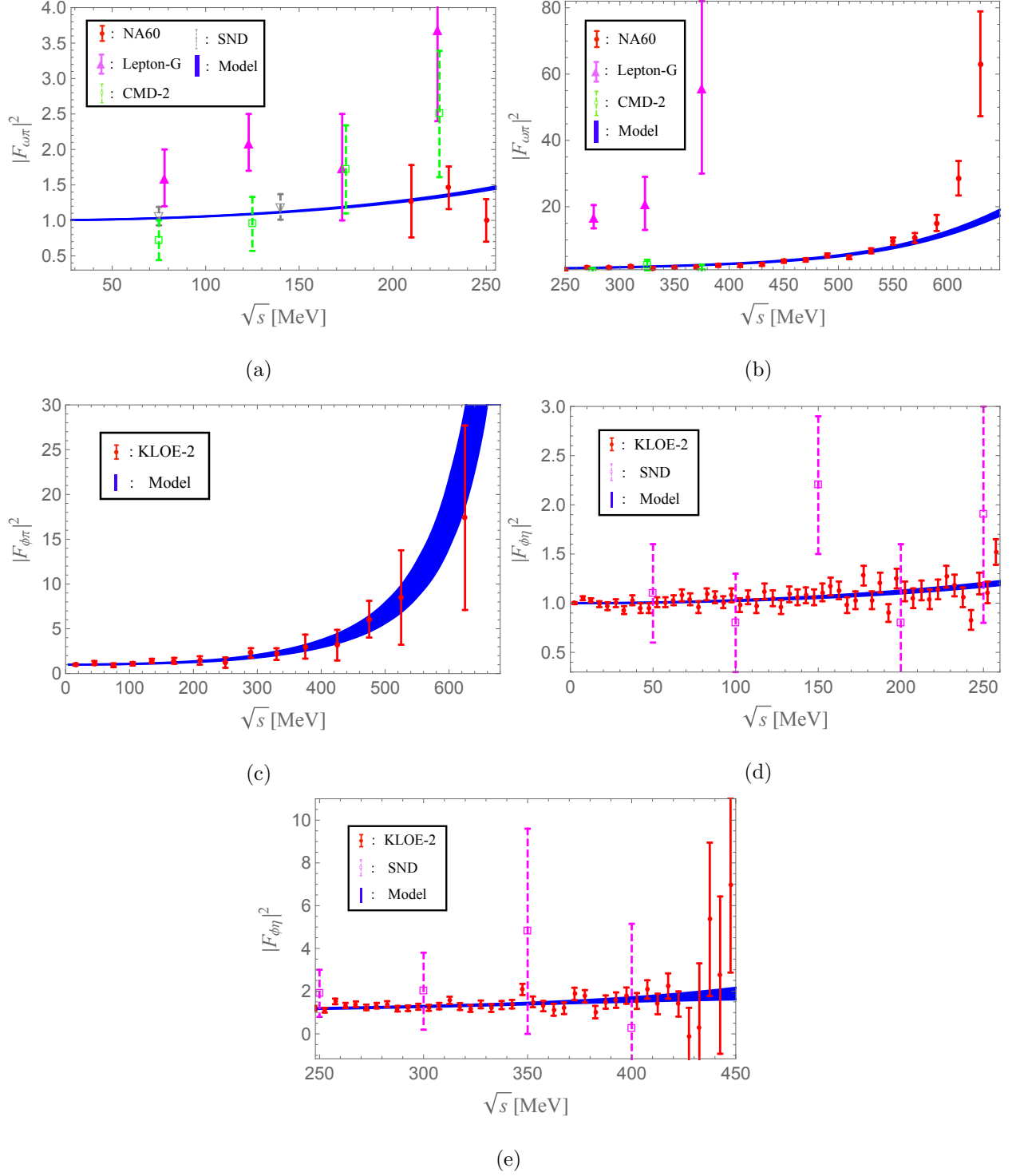


FIG. IV.1. TFFs versus di-lepton invariant mass: (a)-(b) $\omega \rightarrow \pi^0 l^+ l^-$ in the ranges for [30, 250], and [250, 650] respectively, (c)-(d) $\phi \rightarrow \eta l^+ l^-$ in the ranges for $[2m_e, 250]$ and [250, 450] respectively and (e) $\phi \rightarrow \pi^0 l^+ l^-$. The blueish bands imply the model values in 68% C.L. For comparison, experimental data are exhibited for (a)-(b) NA60[1], SND[24], Lepton-G[25] and CMD-2[26], (c) KLOE-2[27], (d)-(e) SND[28] and KLOE-2[29].

TABLE VI. The results of the decay widths for $V \rightarrow PP$.

Decay mode	Theory (MeV)	PDG (MeV)
$\Gamma[\omega \rightarrow \pi\pi]$	4.53	0.130 ± 0.016
$\Gamma[\phi \rightarrow K^+K^-]$	2.867	2.086 ± 0.026
$\Gamma[\phi \rightarrow K^0\bar{K}^0]$	1.86887	1.459 ± 0.020

TABLE VII. Model parameters determined in the fittings.

M_V	690MeV	c_3^{IP}	$(1.80 \pm 0.08) \times 10^{-2}$	c_7^{IP}	-0.6 ± 1.8
g	4.8	c_4^{IP}	$(-4.0 \pm 0.2) \times 10^{-2}$	c_8^{IP}	$(-8.4 \pm 0.3) \times 10^{-2}$
L_4^r	7.4×10^{-4}	c_5^{IP}	$(7.0 \pm 0.2) \times 10^{-2}$	c_9^{IP}	0.27 ± 0.40
L_5^r	3.0×10^{-3}	c_6^{IP}	-0.78 ± 0.97	c_{10}^{IP}	$(-5.8 \pm 9.8) \times 10^{-2}$

B. Model prediction

In this subsection, we perform the numerical analysis with the model parameters summarized in Table VII. The partial decay widths of IP violating modes and Dalitz decay distributions are predicted for light hadrons. The model predictions for the partial decay widths are exhibited in Table VIII, and ones for the TFFs of $P^i \rightarrow l^+l^-\gamma$ are shown in Fig.IV.2. The differential decay widths for $P^i \rightarrow \pi^+\pi^-\gamma$ are displayed in Fig.IV.3. For comparison, experimental data[30], which is originally given as arbitrary unit, are also exhibited for $\eta \rightarrow \pi^+\pi^-\gamma$. As for the Dalitz distributions for $V^I \rightarrow P^i l^+l^-$, we plot the 1σ range of model prediction in Table IV.4. In the vicinity of the peak region, plots of the TFFs are exhibited for (a) $\phi \rightarrow \pi^0 l^+l^-$ and (b) $\eta' \rightarrow \gamma l^+l^-$ in Fig.IV.5. The partial contributions from ρ and ω are also indicated in the figures. In (b), one can find that contribution from ω pole is dominant around the region of resonance. It is noteworthy that the peak in (a) is composed of the contribution from $\rho - \omega$ system and the effect of interference is sizable.

TABLE VIII. Partial decay widths of IPV decay mode. For comparison, the value obtained by BES III[2] is shown for $\Gamma[\eta' \rightarrow e^+e^-\gamma]$ and PDG data[23] are written for other decay modes with 1σ errors. We fixed $c_{123} = 0.30$ to minimize χ^2 with respect to the partial widths of $V^I \rightarrow 3\pi$. For theoretical values of $V^I \rightarrow 3\pi, \phi \rightarrow \omega\pi^0$ and $V^I \rightarrow P^i l^+ l^-$, error ranges as 68% C.L. are shown with $c_3^{\text{IP}} = (1.80 \pm 0.08) \times 10^{-2}, c_4^{\text{IP}} = -(4.0 \pm 0.2) \times 10^{-2}, c_6^{\text{IP}} = -0.78 \pm 0.97$ and $c_7^{\text{IP}} = -0.6 \pm 1.8$.

Decay mode	Theory (MeV)	Exp. (MeV)	Ref.
$\Gamma[\pi^0 \rightarrow e^+e^-\gamma]$	9.1×10^{-8}	$(9.1 \pm 0.3) \times 10^{-8}$	[23]
$\Gamma[\eta \rightarrow e^+e^-\gamma]$	8.6×10^{-6}	$(9.0 \pm 0.6) \times 10^{-6}$	[23]
$\Gamma[\eta \rightarrow \mu^+\mu^-\gamma]$	4.2×10^{-7}	$(4.1 \pm 0.6) \times 10^{-7}$	[23]
$\Gamma[\eta' \rightarrow \mu^+\mu^-\gamma]$	1.9×10^{-5}	$(2.1 \pm 0.6) \times 10^{-5}$	[23]
$\Gamma[\eta' \rightarrow e^+e^-\gamma]$	9.32×10^{-5}	$(9.28 \pm 0.95) \times 10^{-5}$	[2]
$\Gamma[\eta \rightarrow \pi^+\pi^-\gamma]$	3.2×10^{-5}	$(5.5 \pm 0.2) \times 10^{-5}$	[23]
$\Gamma[\eta' \rightarrow \pi^+\pi^-\gamma]$	2.2×10^{-2}	$(5.8 \pm 0.3) \times 10^{-2}$	[23]
$\Gamma[\phi \rightarrow \omega\pi^0]$	$(8_{-7}^{+30}) \times 10^{-4}$	$(2.0 \pm 0.2) \times 10^{-4}$	[23]
$\Gamma[\rho^0 \rightarrow \pi^0 e^+e^-]$	$(8.33_{-0.04}^{+0.05}) \times 10^{-4}$	$< 6.0 \times 10^{-3}$	[23]
$\Gamma[\rho^0 \rightarrow \pi^0 \mu^+\mu^-]$	$(9.7_{-0.3}^{+0.4}) \times 10^{-5}$	—	-
$\Gamma[\rho^0 \rightarrow \eta e^+e^-]$	$(3.28 \pm 0.06) \times 10^{-4}$	—	-
$\Gamma[\rho^0 \rightarrow \eta \mu^+\mu^-]$	$(4.5_{-1.2}^{+1.4}) \times 10^{-8}$	—	-
$\Gamma[\omega \rightarrow \pi^0 e^+e^-]$	$(6.70 \pm 0.04) \times 10^{-3}$	$(6.5 \pm 0.5) \times 10^{-3}$	[23]
$\Gamma[\omega \rightarrow \pi^0 \mu^+\mu^-]$	$(0.89 \pm 0.03) \times 10^{-3}$	$(1.1 \pm 0.3) \times 10^{-3}$	[23]
$\Gamma[\omega \rightarrow \eta e^+e^-]$	$(2.9 \pm 0.1) \times 10^{-5}$	—	-
$\Gamma[\omega \rightarrow \eta \mu^+\mu^-]$	$(1.2_{-0.4}^{+0.6}) \times 10^{-8}$	—	-
$\Gamma[\phi \rightarrow \pi^0 e^+e^-]$	$(7.2_{-0.7}^{+0.9}) \times 10^{-5}$	$(4.8 \pm 1.2) \times 10^{-5}$	[23]
$\Gamma[\phi \rightarrow \pi^0 \mu^+\mu^-]$	$(3.4_{-0.7}^{+0.8}) \times 10^{-5}$	—	-
$\Gamma[\phi \rightarrow \eta e^+e^-]$	$(4.40 \pm 0.01) \times 10^{-4}$	$(4.9 \pm 0.4) \times 10^{-4}$	[23]
$\Gamma[\phi \rightarrow \eta \mu^+\mu^-]$	$(2.43 \pm 0.05) \times 10^{-5}$	$< 4.0 \times 10^{-5}$	[23]
$\Gamma[\phi \rightarrow \eta' e^+e^-]$	$(1.3800 \pm 0.0004) \times 10^{-6}$	—	-
$\Gamma[\rho \rightarrow \pi^0 \pi^+ \pi^-]$	$(7.5 \pm 1.3) \times 10^{-3}$	$(1.5 \pm 1.3) \times 10^{-2}$	[23]
$\Gamma[\omega \rightarrow \pi^0 \pi^+ \pi^-]$	$0.97_{-0.12}^{+0.13}$	7.57 ± 0.09	[23]
$\Gamma[\phi \rightarrow \pi^0 \pi^+ \pi^-]$	$0.95_{-0.19}^{+0.28}$	0.65 ± 0.02	[23]

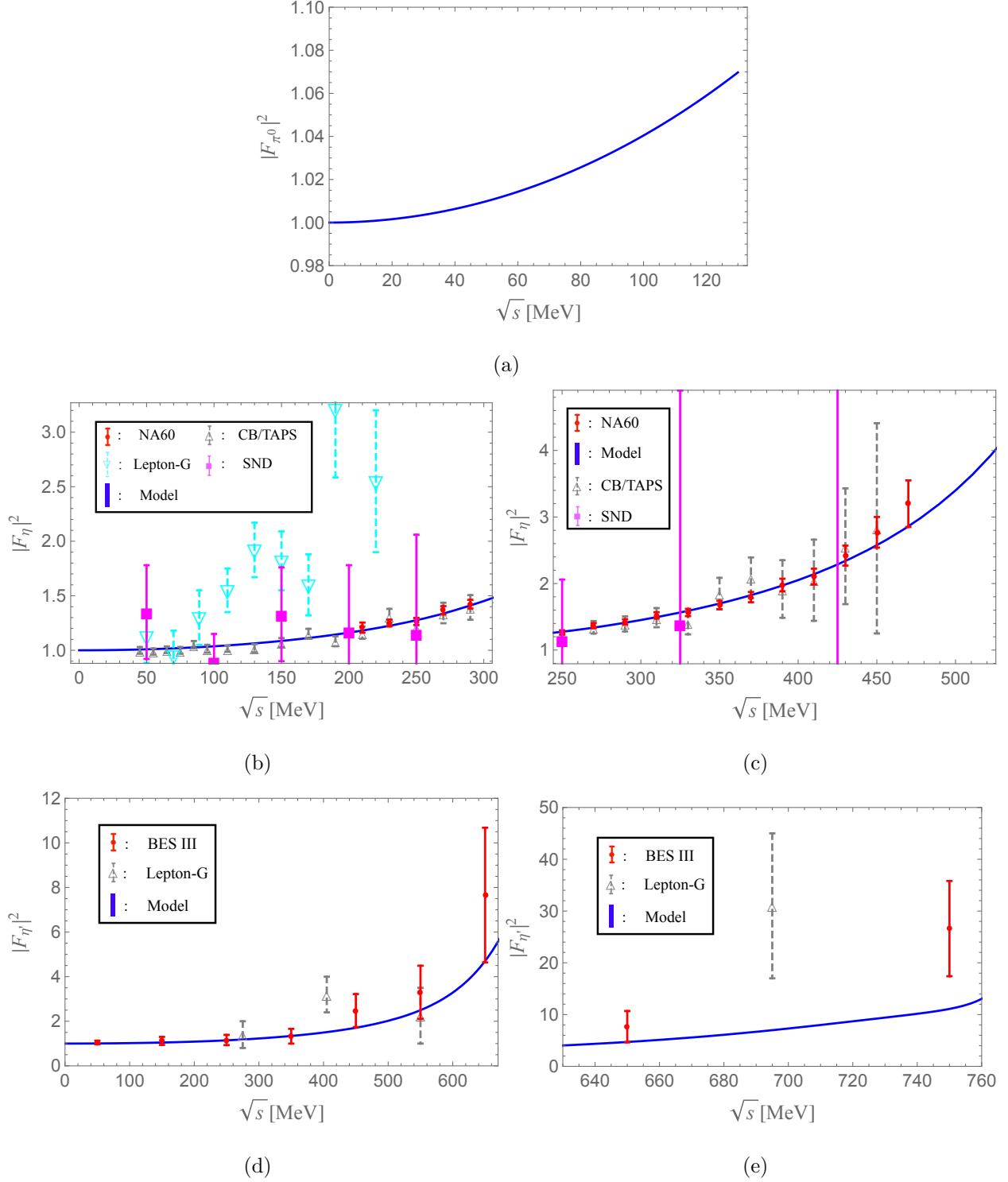


FIG. IV.2. TFFs versus di-lepton invariant mass: (a) $\pi^0 \rightarrow \gamma l^+ l^-$, (b)-(c) $\eta \rightarrow \gamma l^+ l^-$ in the mass range for $[2m_e, 300]$ and for $[250, 520]$ respectively and (d)-(e) $\eta' \rightarrow \gamma l^+ l^-$ in the mass range for $[2m_e, 660]$ and $[620, 760]$ respectively. The blueish curves imply theoretical prediction, we show the experimental data obtained in (b)-(c) NA60[1], Lepton-G[31], CB/TAPS[32] and SND[28] and (d)-(e) BES III[2], Lepton-G[33].

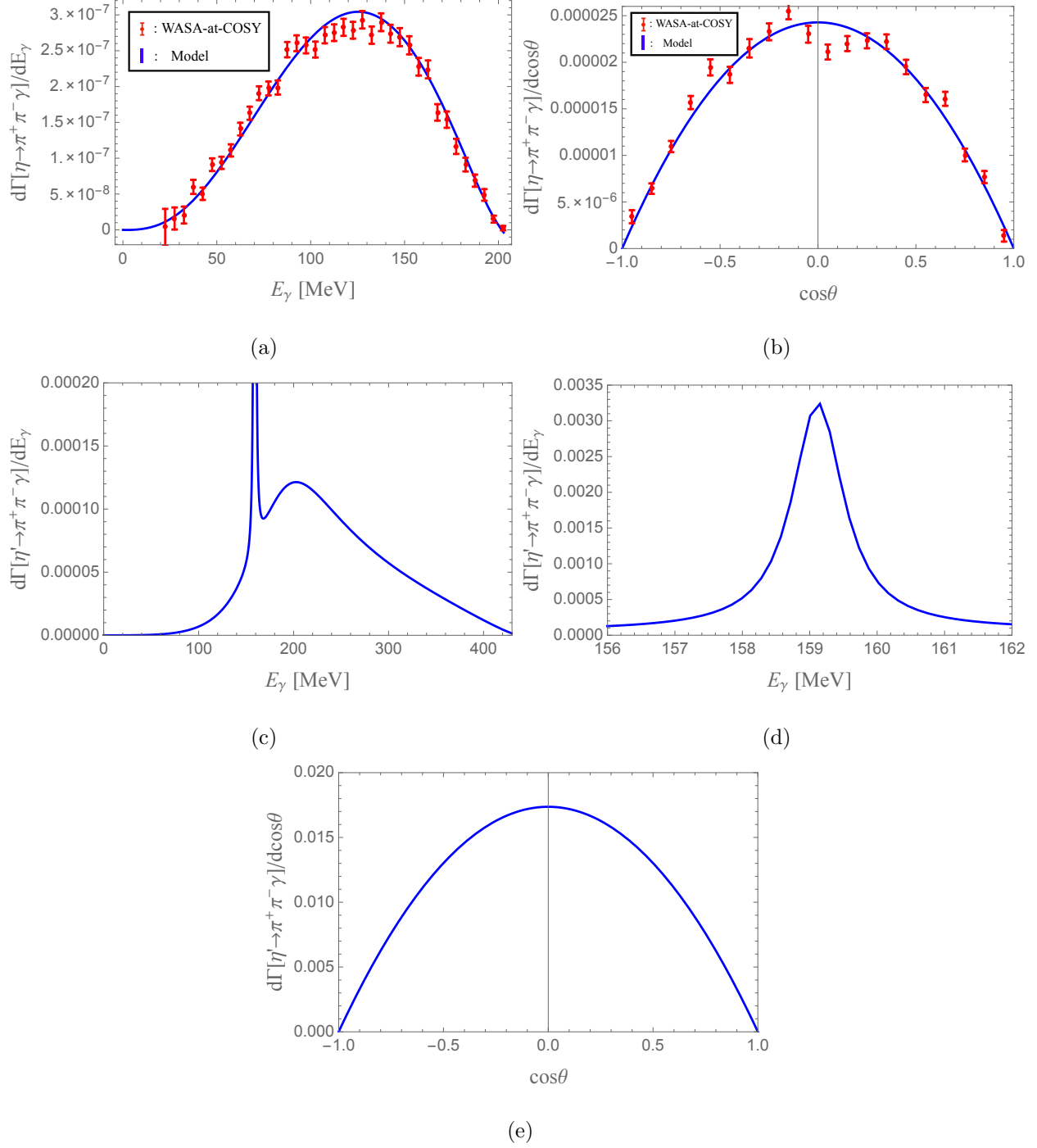


FIG. IV.3. Plots of differential decay width of $P \rightarrow \pi^+\pi^-\gamma$: (a), (c) the distribution of photon energy in the rest frame of $\eta^{(\prime)}$ for decays of η and η' , respectively, (b), (e) the distribution of cosine of the angle between π^+ and γ in the rest frame of $\pi^+\pi^-$ for decays of η and η' , respectively, and (d) the same plot as (c) with magnifying the resonance region. For comparison, the data obtained by WASA-at-COSY collaboration[30] are shown as reddish circles in (a)-(b). Note that we multiplied WASA-at-COSY data (including central values and 1σ errors) by 4.06×10^{-11} in (a) and 2.01×10^{-9} in (b), since their data are recorded in arbitrary unit.

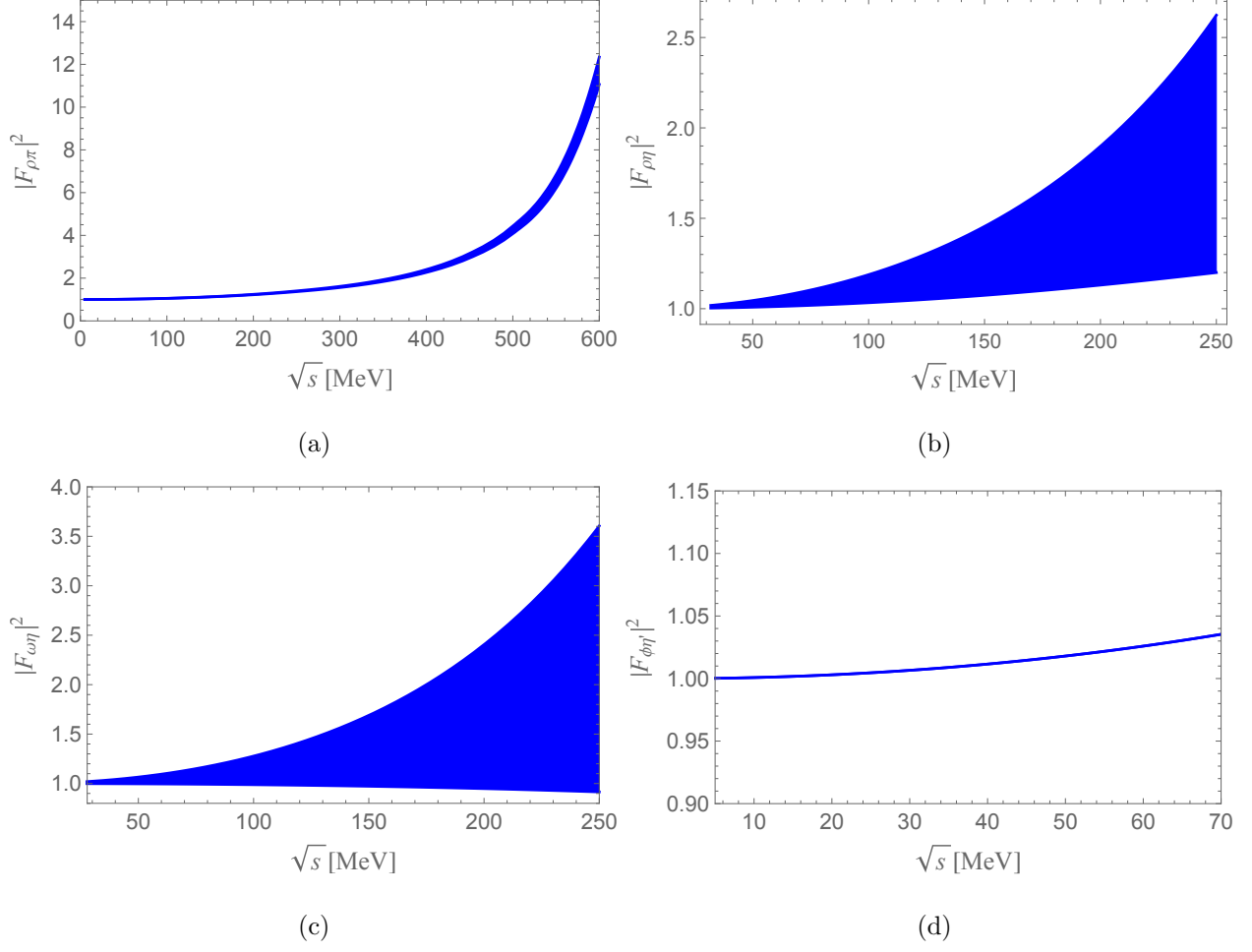
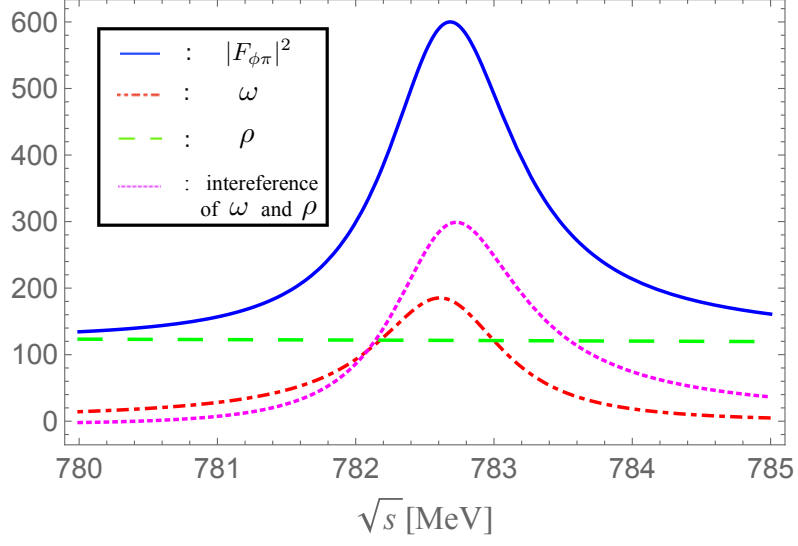
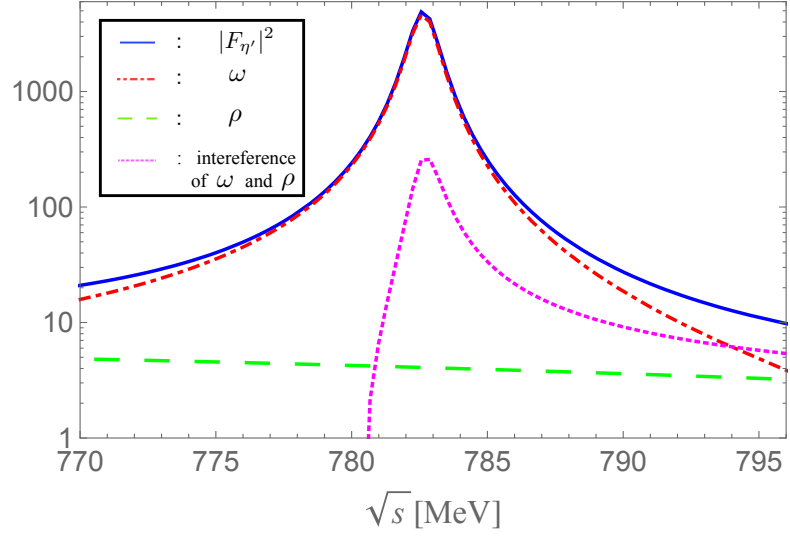


FIG. IV.4. Prediction of the model for TFFs: (a) $\rho^0 \rightarrow \pi^0 l^+ l^-$, (b) $\rho^0 \rightarrow \eta l^+ l^-$, (c) $\omega \rightarrow \eta l^+ l^-$ and (d) $\phi \rightarrow \eta' l^+ l^-$. The blueish bands imply model prediction in 1σ ranges with the model parameters: $c_3^{\text{IP}} = (1.80 \pm 0.08) \times 10^{-2}$, $c_4^{\text{IP}} = -(4.0 \pm 0.2) \times 10^{-2}$, $c_6^{\text{IP}} = -0.78 \pm 0.97$ and $c_7^{\text{IP}} = -0.6 \pm 1.8$.



(a)



(b)

FIG. IV.5. TFFs versus di-lepton invariant mass in the vicinity of the resonance region: (a) $\phi \rightarrow \pi^0 l^+ l^-$ and (b) $\eta' \rightarrow \gamma l^+ l^-$. The blueish solid lines imply the TFFs, and the other lines indicate the partial contribution of intermediate vector mesons.

V. SUMMARY AND DISCUSSION

The IP violating phenomena of light hadrons are investigated with the model of $R\chi PT$. We introduced the suitable tree level interaction Lagrangian which includes singlet fields of vector meson and pseudoscalar. Power counting of superficial degree of divergence enables us to specify the 1-loop order interaction Lagrangian under the presence of the tree level part. With introduced 1-loop interactions, the self-energies of vector mesons are calculated to analyze the processes of hadronic decays.

The analytic formulae are given for the IP violating (differential) decay widths. The calculation with the TFFs of $P \rightarrow \gamma l^+ l^-$ and $V \rightarrow P l^+ l^-$ has been completed in the model of $R\chi PT$. Based on the framework incorporating octet and singlet fields, the IP violating operators are introduced. We constructed $\mathcal{L}_i (i = 5 - 10)$, which consists of the $SU(3)$ singlet fields denoted as η_0 and ϕ_μ^0 . To make the model consistent with the experimental data, the singlet-induced operators play an important role; if $\mathcal{L}_i (i = 5 - 10)$ were absent in the model, $\Gamma[\eta' \rightarrow 2\gamma]$ would become much smaller than the observed value in the experiments.

We found that the electromagnetic TFFs of $\omega \rightarrow \pi^0 l^+ l^-$, $\phi \rightarrow \pi^0 l^+ l^-$ and $\phi \rightarrow \eta l^+ l^-$ are consistent with the experimental data. For the coefficient of the IP violating operators, $c_i (i = 3 - 10)$, the preferred ranges are estimated with χ^2 fitting. The predictions are obtained for the TFFs of $\rho \rightarrow \pi^0 l^+ l^-$, $\rho \rightarrow \eta l^+ l^-$, $\omega \rightarrow \eta l^+ l^-$ and $\phi \rightarrow \eta' l^+ l^-$, which are expected be observed in future experiments. Furthermore, we found that the resonance appears in the TFF of $\eta' \rightarrow \gamma l^+ l^-$ due to the contribution from the pole for ω . Remarkably, the peak in the TFF of $\phi \rightarrow \pi^0 l^+ l^-$ consists of the effect of interference between ρ and ω , unlike one for $\eta' \rightarrow \gamma l^+ l^-$. Finally, we comment on the disagreement of $\Gamma[\omega \rightarrow \pi^+ \pi^- \pi^0]$ and $\Gamma[\omega \rightarrow \pi^+ \pi^-]$. Since the process of $\omega \rightarrow \pi^+ \pi^-$ violates G-parity, taking account of isospin breaking is important. It is expected that improvement will be presumably shown with higher order correction of isospin breaking.

Appendix A: Counter terms

The counter terms are computed with 1-loop correction of $SU(3)$ singlet pseudoscalar in Ref.[18]. In this work, we only consider the corrections due to $SU(3)$ octet pseudoscalars. The effect of $SU(3)_R$ external gauge boson is included. The counter terms in 1-loop order

are,

$$\begin{aligned}
\mathcal{L}_c = & L_1 (\text{Tr}(D_\mu U (D^\mu U)^\dagger))^2 + L_2 \text{Tr}(D_\mu U (D_\nu U)^\dagger) \text{Tr}(D^\mu U (D^\nu U)^\dagger) \\
& + L_3 \text{Tr}\{D^\mu U (D_\mu U)^\dagger D^\nu U (D_\nu U)^\dagger\} \\
& + \frac{4B}{f^2} L_4 \text{Tr}\{D_\mu U (D^\mu U)^\dagger\} \text{Tr}\{M(U + U^\dagger)\} \\
& + \frac{4B}{f^2} L_5 \text{Tr}\{D_\mu U (D^\mu U)^\dagger (UM + MU^\dagger)\} \\
& + \frac{16B^2}{f^4} L_6 \{\text{Tr}(M(U + U^\dagger))\}^2 \\
& + \frac{16B^2}{f^4} L_7 \{\text{Tr}(M(U - U^\dagger))\}^2 \\
& + \frac{16B^2}{f^4} L_8 \text{Tr}(MUMU + MU^\dagger MU^\dagger) \\
& + iL_9 \text{Tr}\{F_{L\mu\nu} (D^\mu U) (D^\nu U)^\dagger + F_{R\mu\nu} (D^\mu U)^\dagger D^\nu U\} \\
& + L_{10} \text{Tr}(F_{L\mu\nu} U F_R^{\mu\nu} U^\dagger) \\
& + H_1 \text{Tr}(F_{L\mu\nu} F_L^{\mu\nu} + F_{R\mu\nu} F_R^{\mu\nu}) \\
& + H_2 \left(\frac{4B}{f^2}\right)^2 \text{Tr}(M^2) \\
& + i\frac{K_1}{2} \text{Tr}(\xi^\dagger D^\mu U (D^\nu U)^\dagger \xi) (D_\mu v_\nu - D_\nu v_\mu + i[v_\mu, v_\nu]) \\
& - \frac{1}{2} (K_2 \text{Tr}(\xi^\dagger F_{L\mu\nu} \xi + \xi F_{R\mu\nu} \xi^\dagger) (D^\mu v^\nu - D^\nu v^\mu + i[v^\mu, v^\nu]) \\
& + K_3 \text{Tr}(D_\mu v_\nu - D_\nu v_\mu + i[v_\mu, v_\nu]) (D^\mu v^\nu - D^\nu v^\mu + i[v^\mu, v^\nu])) \\
& + \frac{4B}{f^2} (K_4 \text{Tr}\{(\xi M \xi + \xi^\dagger M \xi^\dagger) v^2\} + K_5 \text{Tr}\{M(U + U^\dagger)\} \text{Tr}(v^2)) \\
& + K_6 \text{Tr}(v_\rho \alpha_\perp^\mu) \text{Tr}(v^\rho \alpha_{\perp\mu}) + K_7 \text{Tr}(v^2 \alpha_{\perp\mu} \alpha_\perp^\mu) + K_8 \text{Tr}(\alpha_\perp^2) \text{Tr}(v^2) \\
& + K_9 \{\text{Tr}(v^2)\}^2 + K_{10} \text{Tr}(v^4) \\
& + i\frac{g_{2p}}{f^2} T_1 \eta_0 \text{Tr}\{(\xi M \xi - \xi^\dagger M \xi^\dagger) v^2\} \\
& + i\frac{g_{2p}}{f^2} T_2 \eta_0 \text{Tr}\{M(U - U^\dagger)\} \text{Tr}(v^2) \\
& + T_3 i\frac{g_{2p}}{f^2} \frac{4B}{f^2} \eta_0 \text{Tr}M(U + U^\dagger) \text{Tr}M(U - U^\dagger) \\
& + T_4 \left(\frac{g_{2p}}{f^2}\right)^2 \eta_0^2 (\text{Tr}M(U - U^\dagger))^2 + iT_5 \frac{4B}{f^2} \frac{g_{2p}}{f^2} \eta_0 \text{Tr}(MUMU - MU^\dagger MU^\dagger) \\
& + T_6 \left(\frac{g_{2p}}{f^2}\right)^2 \eta_0^2 \text{Tr}(MUMU + MU^\dagger MU^\dagger - 2M^2) \\
& + i\frac{g_{2p}}{f^2} \eta_0 [T_7 \text{Tr}\{M(D_\mu U (D^\mu U)^\dagger U - U^\dagger D_\mu U (D^\mu U)^\dagger)\} \\
& + T_8 \text{Tr}(M(U - U^\dagger)) \text{Tr}(D_\mu U (D^\mu U)^\dagger)], \tag{A1}
\end{aligned}$$

$$v_\mu = g_{\rho\pi\pi} \left(V_\mu - \frac{\alpha_\mu}{g} \right), \quad (\text{A2})$$

$$L_i = \lambda \Gamma_i + L_i^r (i = 1 - 10), \quad (\text{A3})$$

$$K_i = \lambda k_i + K_i^r (i = 1 - 10), \quad (\text{A4})$$

$$H_i = \lambda \Delta_i + H_i^r (i = 1 - 2), \quad (\text{A5})$$

$$T_i = \lambda t_i + T_i^r (i = 1 - 8), \quad (\text{A6})$$

$$\lambda = -\frac{1}{32\pi^2} (1 + C_{UV} - \ln \mu^2), \quad (\text{A7})$$

$$C_{UV} = \frac{1}{2 - \frac{d}{2}} - \gamma + \ln 4\pi. \quad (\text{A8})$$

In Eq.(A1), the contribution from singlet pseudoscalar is omitted in the coefficients of Γ_6, Γ_8 and Δ_2 . We have also corrected the sign of k_9 and k_{10} in Ref.[18].

TABLE IX. The coefficients of the counter terms: k_i, Γ_i and Δ_i .

$k_1 = 1$	$t_1 = -6$	$\Gamma_1 = \frac{2c^2+1}{32}$	$\Delta_1 = -\frac{1}{8}$
$k_2 = 1$	$t_2 = -2$	$\Gamma_2 = \frac{1+2c^2}{16}$	$\Delta_2 = \frac{5}{24}$
$k_3 = 1$	$t_3 = -\frac{11}{18}$	$\Gamma_3 = \frac{3(c^2-1)}{16}$	
$k_4 = \frac{3}{2}$	$t_4 = -\frac{11}{9}$	$\Gamma_4 = \frac{c}{8}$	
$k_5 = \frac{1}{2}$	$t_5 = -\frac{5}{6}$	$\Gamma_5 = \frac{3c}{8}$	
$k_6 = 4c$	$t_6 = -\frac{5}{3}$	$\Gamma_6 = \frac{11}{144}$	
$k_7 = 6c$	$t_7 = -\frac{3c}{2}$	$\Gamma_7 = 0$	
$k_8 = 2c$	$t_8 = -\frac{c}{2}$	$\Gamma_8 = \frac{5}{48}$	
$k_9 = 3$		$\Gamma_9 = \frac{1}{4}$	
$k_{10} = 3$		$\Gamma_{10} = -\frac{1}{4}$	

Appendix B: Power counting with SU(3) breaking and singlets

In this appendix, we show the power counting rule which is used to classify the interaction Lagrangian and counter terms in Eq.(1). The divergence of the chiral corrections within 1-loop is computed in Ref.[18] for the chiral Lagrangian with vector meson octet and the counter terms which subtract the divergence are obtained. The types of the counter terms are determined by the forms predicted by the power counting rule. Therefore with the power

counting, one can systematically include the higher loop chiral corrections. Although the power counting is applied to the interaction terms among pseudoscalar octets and the others, it does not apply to the kinetic term of the vector meson octets, pseudoscalar and vector meson singlets. We choose the canonical kinetic terms for the singlets. The kinetic term of the non-Abelian type is adopted for the vector meson octets [3, 10].

In general, the power counting rule is obtained by computing the superficial degree of divergence of the amplitude. If the degree is non-negative, the power of the degree corresponds to the number of the derivative included in the counter term. In the previous paper, [18], we studied the superficial degree of divergence for chiral corrections in one particle irreducible (1 PI) part of the effective chiral Lagrangian with vector mesons. The degree ω is computed in the chiral limit as,

$$\omega = 2N_L + 2 - N_{V_8}, \quad (\text{B1})$$

where N_L is a number of loop and N_{V_8} is a number of the external line of the octet vector mesons. Since the sum $\omega + N_{V_8}$ is a constant for a fixed number of loop N_L , it implies an external octet vector meson is equivalent to the first derivative from the view point of the power counting. In this work, we extend the power counting formula to the case with chiral breaking terms under the presence of SU(3) singlet vector and pseudoscalar mesons. We first examine the Lagrangian in Eq.(1) from the view point of the power counting. The octet vector meson couplings to octet pseudoscalars are given as a part of the chiral invariant mass term for vector meson octet,

$$M_V^2 \text{Tr} \left(V_\mu - \frac{\alpha_\mu}{g} \right) \left(V^\mu - \frac{\alpha^\mu}{g} \right). \quad (\text{B2})$$

Since this term includes the interaction of pseudoscalars with two first derivatives, one can classify it as a leading order interaction. With an insertion of the chiral breaking $\xi M \xi + h.c.$, one can write the following terms,

$$\begin{aligned} & C_1 \frac{2B}{f^2} \text{Tr} \left\{ (\xi M \xi + \xi^\dagger M \xi^\dagger) \left(V_\mu - \frac{\alpha_\mu}{g} \right) \left(V^\mu - \frac{\alpha^\mu}{g} \right) \right\} \\ & + C_2 \frac{2B}{f^2} \text{Tr} (\xi M \xi + \xi^\dagger M \xi^\dagger) \text{Tr} \left\{ \left(V_\mu - \frac{\alpha_\mu}{g} \right) \left(V^\mu - \frac{\alpha^\mu}{g} \right) \right\}. \end{aligned} \quad (\text{B3})$$

These terms include an insertion of the chiral breaking and are suppressed by a factor $O(\xi M \xi + h.c.) = O(m_\pi^2)$, compared with a term without an insertion of Eq.(B2). We regard them as 1-loop order counter terms. Next we consider the interaction of the pseudoscalar

singlet and pseudoscalar octets. Although one may consider a chiral invariant term with two first derivatives, it vanishes,

$$\partial_\mu \eta^0 \text{Tr}(\alpha_\perp^\mu) = 0, \quad (\text{B4})$$

because of the traceless property of α_\perp . The following term proportional to the chiral breaking,

$$-ig_{2p}\eta^0 \text{Tr}M(U - U^\dagger), \quad (\text{B5})$$

does not vanish and this term is included in the leading order Lagrangian. The chiral invariant interaction of the singlet vector meson to the octet pseudoscalars also vanishes,

$$\phi^{0\mu} \text{Tr} \left(V_\mu - \frac{\alpha_\mu}{g} \right) = 0, \quad (\text{B6})$$

due to the traceless property of $V_\mu - \frac{\alpha_\mu}{g}$. The non-vanishing contribution of the singlet vector meson is given as,

$$g_{1V}\phi^{\mu 0} \text{Tr}(\xi M \xi + \xi^\dagger M \xi^\dagger) \left(V_\mu - \frac{\alpha_\mu}{g} \right). \quad (\text{B7})$$

We assume that both vector meson octets and singlet are the same order as the first derivative. Since Eq.(B7) also includes two vector meson fields and a chiral breaking insertion, it is a 1-loop order term. In contrast to Eq.(B5) of the singlet pseudoscalar, the leading contribution of the singlet vector meson is counted as 1-loop order. Based upon the consideration, the tree level Lagrangian is given in Eq.(12). The superficial degree of divergence for N_L loop diagrams with Eq.(12) is given as,

$$\omega_0 = 2N_L + 2 - N_{V_8} - N_\chi - N_{\eta_0}, \quad (\text{B8})$$

where N_χ is the number of the chiral breaking insertion and N_{η_0} is the number of the external line for η_0 . We treat the chiral breaking term proportional to B as interaction and the propagator of pseudoscalar octets is given as $\frac{1}{p^2}$. We will give the proof of Eq.(B8) below. If the number of the vertices is N_v and the number of the internal propagators for pseudoscalar octets is N_I , the number of the chiral invariant vertex with two derivatives is given as,

$$N_{v2} = N_v - (N_{V_8} + N_\chi + N_{\eta_0}) \quad (\text{B9})$$

and the number of the independent loop is,

$$N_L = N_I - (N_v - 1). \quad (\text{B10})$$

The superficial degree of divergence is obtained with the relation,

$$p^{\omega_0} = p^{4N_L} \left(\frac{1}{p^2} \right)^{N_I} (p^2)^{N_{v2}} p^{N_{V_8}}, \quad (\text{B11})$$

$$\omega_0 = 4N_L - 2N_I + 2N_{v2} + N_{V_8} = 2N_L + 2 - 2(N_\chi + N_{\eta_0}) - N_{V_8}. \quad (\text{B12})$$

The form of the counter term is,

$$\partial^{\omega_0} M^{N_\chi + N_{\eta_0}} \eta_0^{N_{\eta_0}} V_8^{N_{V_8}}. \quad (\text{B13})$$

Let us examine the counter terms given in Eq.(A1) in 1-loop order using the superficial degree of divergence,

$$\omega_0(N_L = 1) = 4 - 2(N_\chi + N_{\eta_0}) - N_{V_8}. \quad (\text{B14})$$

In Table X, we show the number of the derivative ω_0 , the number of insertion of the chiral breaking term N_χ , the number of pseudoscalar singlet N_{η_0} and the number of the vector meson octets N_{V_8} in each 1-loop counter term. We classify each counter term according to these numbers and show their coefficients. Although the counter terms which subtract the divergence of 1-loop have the forms expected from the power counting in Eqs.(B13, B14), they do not complete all the interactions which are needed in 1-loop order calculation. Such terms include the singlet vector meson interaction in Eq.(B7) and one treats it as a finite counter term. We also need to add the following chiral invariant term with a singlet pseudoscalar,

$$\partial_\mu \eta^0 \text{Tr}(\alpha_\perp \cdot \alpha_\perp \alpha_\perp^\mu). \quad (\text{B15})$$

It contains the fourth derivatives. Intrinsic parity violating terms in \mathcal{L}_{IPV} should be also included as finite counter terms.

TABLE X. $(\omega_0, N_\chi, N_{\eta_0}, N_{V_8})$ for 1-loop counter terms.

ω_0	N_χ	N_{η_0}	N_{V_8}	The coefficients of the counter terms
4	0	0	0	$L_1, L_2, L_3, L_9, L_{10}, H_1, K_1, K_2, K_3, K_6, K_7, K_8, K_9, K_{10}$
3	0	0	1	$K_1, K_2, K_3, K_6, K_7, K_8, K_9, K_{10}$
2	1	0	0	L_4, L_5, K_4, K_5
0	2	0	0	L_6, L_7, L_8, H_2
2	0	0	2	$K_1, K_2, K_3, K_6, K_7, K_8, K_9, K_{10}$
2	0	1	0	T_1, T_2, T_7, T_8
1	0	1	1	T_1, T_2
0	0	1	2	T_1, T_2
0	1	1	0	T_3, T_5
0	0	2	0	T_4, T_6
0	1	0	2	K_4, K_5
1	1	0	1	K_4, K_5
1	0	0	3	K_3, K_9, K_{10}
0	0	0	4	K_3, K_9, K_{10}

Appendix C: Self-Energy for K^* and charged ρ meson

In this appendix, we study self-energy corrections to K^{*+0} mesons and charged ρ meson taking SU(3) breaking into account. The interaction Lagrangian for $V \rightarrow PP$ is given as,

$$\begin{aligned}
 \mathcal{L}^{VPP} &= -\frac{2g_{\rho\pi\pi}}{i} \text{Tr}(V_\mu[\Delta, \partial^\mu \Delta]) \\
 &= i\frac{g_{\rho\pi\pi}}{2} \left[K^{*+\mu} \left(\hat{K}^- \overset{\leftrightarrow}{\partial}_\mu \hat{\pi}_3 + \sqrt{3} \hat{K}^- \overset{\leftrightarrow}{\partial}_\mu \hat{\eta}_8 + \sqrt{2} \hat{K}^0 \overset{\leftrightarrow}{\partial}_\mu \hat{\pi}^- \right) \right. \\
 &\quad + K^{*0\mu} \left(-\hat{K}^0 \overset{\leftrightarrow}{\partial}_\mu \hat{\pi}_3 + \sqrt{3} \hat{K}^0 \overset{\leftrightarrow}{\partial}_\mu \hat{\eta}_8 + \sqrt{2} \hat{K}^- \overset{\leftrightarrow}{\partial}_\mu \hat{\pi}^- \right) \\
 &\quad \left. + \rho^{+\mu} \left(2\hat{\pi}^- \overset{\leftrightarrow}{\partial}_\mu \hat{\pi}_3 + \sqrt{2} \hat{K}^0 \overset{\leftrightarrow}{\partial}_\mu \hat{K}^- \right) \right] + h.c., \tag{C1}
 \end{aligned}$$

$$\Delta = \frac{1}{2} \begin{pmatrix} \hat{\pi}_3 + \frac{\hat{\eta}_8}{\sqrt{3}} & \sqrt{2}\hat{\pi}^+ & \sqrt{2}\hat{K}^+ \\ \sqrt{2}\hat{\pi}^- & -\hat{\pi}_3 + \frac{\hat{\eta}_8}{\sqrt{3}} & \sqrt{2}\hat{K}^0 \\ \sqrt{2}\hat{K}^+ & \sqrt{2}\hat{K}^0 & -2\frac{\hat{\eta}_8}{\sqrt{3}} \end{pmatrix}, \tag{C2}$$

where Δ denotes the quantum fluctuation for the pseudoscalar octet in the background field method [18]. The isospin breaking leads to $\pi_3 - \eta_8$ mixing and the Feynman diagrams for the self-energy of K^{*+0} are shown in Fig.C.1. $\pi_3 - \eta_8$ mixing obtained from the chiral breaking

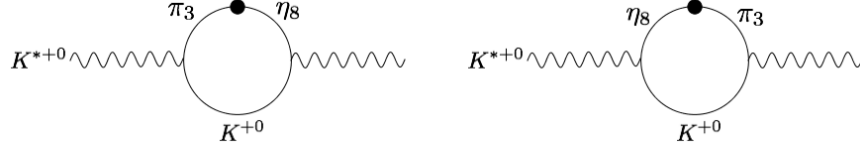


FIG. C.1. Self-energy corrections to K^{*+0} . The diagrams include the $\pi_3 - \eta_8$ mixing due to the isospin breaking effect.

term is given by the following Lagrangian,

$$\mathcal{L} = -M_{38}^2 \hat{\pi}_3 \hat{\eta}_8, \quad (\text{C3})$$

$$M_{38}^2 = \frac{1}{\sqrt{3}}(M_{K^+}^2 - M_{K^0}^2). \quad (\text{C4})$$

We treat the mixing in Eq.(C3) as perturbation. The mixing insertion is denoted with black circles in Fig.C.1. Below, the amplitude corresponding to the diagrams in Fig.C.1 is shown,

$$\begin{aligned} & \frac{g_{\rho\pi\pi}^2}{4} \int \frac{d^d k}{(2\pi)^d i} \frac{(Q-2k)_\mu (Q-2k)_\nu}{((Q-k)^2 - M_\pi^2)((Q-k)^2 - M_{\eta_8}^2)(k^2 - M_K^2)} 2\sqrt{3}M_{38}^2 \\ &= \frac{g_{\rho\pi\pi}^2}{2} \frac{M_{K^+}^2 - M_{K^0}^2}{M_{\eta_8}^2 - M_\pi^2} (J_{\mu\nu}^{\eta_8 K} - J_{\mu\nu}^{\pi^0 K}) \\ &= 2g_{\rho\pi\pi}^2 \frac{M_{K^+}^2 - M_{K^0}^2}{M_{\eta_8}^2 - M_\pi^2} Q_{\mu\nu} (M_{K\eta_8}^r - M_{K\pi}^r) \\ &+ g_{\rho\pi\pi}^2 (M_{K^+}^2 - M_{K^0}^2) g_{\mu\nu} \left(2 \frac{L_{K\eta_8} - L_{K\pi}}{M_{\eta_8}^2 - M_\pi^2} - \lambda - \frac{\mu_{\eta_8} - \mu_\pi}{M_{\eta_8}^2 - M_\pi^2} \right), \end{aligned} \quad (\text{C5})$$

where $Q_{\mu\nu}$ is defined in Eq.(19) and M_K denotes M_{K^+} or M_{K^0} and one uses the following 1-loop function,

$$\begin{aligned} J_{\mu\nu}^{QP} &= \int \frac{d^d k}{(2\pi)^d i} \frac{(Q-2k)_\mu (Q-2k)_\nu}{((Q-k)^2 - M_Q^2)(k^2 - M_P^2)} \\ &= Q_{\mu\nu} \left(4M_{PQ}^r - \frac{2}{3}\lambda \right) + g_{\mu\nu} (4L_{PQ} - 2\lambda\Sigma_{PQ} - 2(\mu_Q + \mu_P)), \end{aligned} \quad (\text{C6})$$

$$\Sigma_{PQ} = M_P^2 + M_Q^2. \quad (\text{C7})$$

In Eqs.(C5, C6), λ denotes the ultraviolet divergence defined in Eq.(A7). In Eq.(C6), L_{PQ} and M_{PQ}^r are functions given below,

$$M_{PQ}^r = \frac{1}{12Q^2} (Q^2 - 2\Sigma_{PQ}) \bar{J}_{PQ} + \frac{\Delta_{PQ}^2}{3Q^4} \left[\bar{J}_{PQ} - Q^2 \frac{1}{32\pi^2} \left(\frac{\Sigma_{PQ}}{\Delta_{PQ}^2} + 2 \frac{M_P^2 M_Q^2}{\Delta_{PQ}^3} \ln \frac{M_Q^2}{M_P^2} \right) \right] - \frac{k_{PQ}}{6} + \frac{1}{288\pi^2}, \quad (\text{C8})$$

$$L_{PQ} = \frac{\Delta_{PQ}^2}{4s} \bar{J}_{PQ}, \quad (\text{C9})$$

$$k_{PQ} = \frac{(\mu_P - \mu_Q) f^2}{\Delta_{PQ}}. \quad (\text{C10})$$

In Eqs.(C8, C9), \bar{J}_{PQ} is a 1-loop scalar function of pseudoscalar mesons with masses M_P and M_Q . Above the threshold $Q^2 \geq (M_P + M_Q)^2$, it is given by,

$$\bar{J}_{PQ}(Q^2) = \frac{1}{32\pi^2} \left[2 + \frac{\Delta_{PQ}}{Q^2} \ln \frac{M_Q^2}{M_P^2} - \frac{\Sigma_{PQ}}{\Delta_{PQ}} \ln \frac{M_Q^2}{M_P^2} - \frac{\nu_{PQ}}{Q^2} \ln \frac{(Q^2 + \nu_{PQ})^2 - \Delta_{PQ}^2}{(Q^2 - \nu_{PQ})^2 - \Delta_{PQ}^2} \right] + \frac{i}{16\pi} \frac{\nu_{PQ}}{Q^2}, \quad (\text{C11})$$

$$\nu_{PQ}^2 = Q^4 - 2Q^2 \Sigma_{PQ} + \Delta_{PQ}^2, \quad (\text{C12})$$

while below the threshold $(M_P - M_Q)^2 \leq Q^2 \leq (M_P + M_Q)^2$,

$$\bar{J}_{PQ}(Q^2) = \frac{1}{32\pi^2} \left[2 + \frac{\Delta_{PQ}}{Q^2} \ln \frac{M_Q^2}{M_P^2} - \frac{\Sigma_{PQ}}{\Delta_{PQ}} \ln \frac{M_Q^2}{M_P^2} - 2 \frac{\sqrt{-\nu_{PQ}^2}}{Q^2} \left(\arctan \frac{Q^2 - \Delta_{PQ}}{\sqrt{-\nu_{PQ}^2}} + \arctan \frac{Q^2 + \Delta_{PQ}}{\sqrt{-\nu_{PQ}^2}} \right) \right]. \quad (\text{C13})$$

We write inverse propagators of vector mesons as,

$$D_{V\mu\nu}^{-1} = (M_V^2 + \delta A_V) g_{\mu\nu} + \delta \tilde{B}_V Q_\mu Q_\nu, \quad (\text{C14})$$

where the metric part of the inverse propagator consists of the sum of tree level mass M_V and loop correction δA_V . Using loop functions defined, we add the isospin breaking corrections in Fig.C.1 to the calculation given in Ref.[18]. We also take account of the mass differences of $K^+ - K^0$ and $\pi^+ - \pi^0$, which were not considered in the previous study. The self-energy

corrections to K^{*+0} and ρ^+ mesons are obtained as,

$$\begin{aligned}\delta\tilde{B}_{K^{*+}} &= Z_V^r(\mu) + g_{\rho\pi\pi}^2 \left[2M_{K^0\pi^+}^r + M_{K^+\pi^0}^r + 3M_{K^+\eta_8}^r + 2\frac{M_{K^+}^2 - M_{K^0}^2}{M_{\eta_8}^2 - M_\pi^2} (M_{K^+\eta_8}^r - M_{K^+\pi^0}^r) \right], \\ \delta A_{K^{*+}} &= \Delta A_{K^{*+}} + C_1^r(\mu)M_{K^+}^2 + C_2^r(\mu)(2\bar{M}_K^2 + M_\pi^2) - Q^2 Z_V^r(\mu),\end{aligned}\quad (C15)$$

$$\begin{aligned}\Delta A_{K^{*+}} &= -Q^2 g_{\rho\pi\pi}^2 \left[2M_{K^0\pi^+}^r + M_{K^+\pi^0}^r + 3M_{K^+\eta_8}^r + 2\frac{M_{K^+}^2 - M_{K^0}^2}{M_{\eta_8}^2 - M_\pi^2} (M_{K^+\eta_8}^r - M_{K^+\pi^0}^r) \right] \\ &+ g_{\rho\pi\pi}^2 \left[2 \left(\frac{M_{K^+}^2 - M_{K^0}^2}{M_{\eta_8}^2 - M_\pi^2} \right) \left(L_{K^+\eta_8} - L_{K^+\pi^0} - \frac{f^2}{2}(\mu_{\eta_8} - \mu_\pi) \right) + 2L_{K^0\pi^+} + L_{K^+\pi^0} \right. \\ &\left. + 3L_{K^+\eta_8} - \frac{f^2}{2} \{ 2(\mu_{K^0} + \mu_\pi) + \mu_{K^+} + \mu_\pi + 3(\mu_{K^+} + \mu_{\eta_8}) \} \right],\end{aligned}\quad (C16)$$

$$\begin{aligned}\delta\tilde{B}_{K^{*0}} &= Z_V^r(\mu) + g_{\rho\pi\pi}^2 \left[2M_{K^+\pi^-}^r + M_{K^0\pi^0}^r + 3M_{K^0\eta_8}^r - 2\frac{M_{K^+}^2 - M_{K^0}^2}{M_{\eta_8}^2 - M_\pi^2} (M_{K^0\eta_8}^r - M_{K^0\pi^0}^r) \right], \\ \delta A_{K^{*0}} &= \Delta A_{K^{*0}} + C_1^r(\mu)M_{K^0}^2 + C_2^r(\mu)(2\bar{M}_K^2 + M_\pi^2) - Q^2 Z_V^r(\mu),\end{aligned}\quad (C17)$$

$$\begin{aligned}\Delta A_{K^{*0}} &= -Q^2 g_{\rho\pi\pi}^2 \left[2M_{K^+\pi^-}^r + M_{K^0\pi^0}^r + 3M_{K^0\eta_8}^r - 2\frac{M_{K^+}^2 - M_{K^0}^2}{M_{\eta_8}^2 - M_\pi^2} (M_{K^0\eta_8}^r - M_{K^0\pi^0}^r) \right] \\ &+ g_{\rho\pi\pi}^2 \left[-2 \left(\frac{M_{K^+}^2 - M_{K^0}^2}{M_{\eta_8}^2 - M_\pi^2} \right) \left(L_{K^0\eta_8} - L_{K^0\pi^0} - \frac{f^2}{2}(\mu_{\eta_8} - \mu_\pi) \right) \right. \\ &\left. + 2L_{K^+\pi^-} + L_{K^0\pi^0} + 3L_{K^0\eta_8} - \frac{f^2}{2} \{ 2(\mu_{K^+} + \mu_\pi) + \mu_{K^0} + \mu_\pi + 3(\mu_{K^0} + \mu_{\eta_8}) \} \right],\end{aligned}\quad (C18)$$

$$\begin{aligned}\delta\tilde{B}_{\rho^+} &= Z_V^r(\mu) + g_{\rho\pi\pi}^2 (4M_{\pi^+\pi^0}^r + 2M_{K^+\bar{K}^0}^r), \\ \delta A_{\rho^+} &= \Delta A_{\rho^+} + C_1^r(\mu)M_\pi^2 + C_2^r(\mu)(2\bar{M}_K^2 + M_\pi^2) - Q^2 Z_V^r(\mu),\end{aligned}\quad (C19)$$

$$\begin{aligned}\Delta A_{\rho^+} &= -Q^2 g_{\rho\pi\pi}^2 (4M_{\pi^+\pi^0}^r + 2M_{K^+\bar{K}^0}^r) \\ &+ 2g_{\rho\pi\pi}^2 \left(2L_{\pi^+\pi^0} + L_{K^+\bar{K}^0} - \frac{f^2}{2} (4\mu_\pi + \mu_{K^+} + \mu_{K^0}) \right).\end{aligned}\quad (C20)$$

Appendix D: Proof of the relation for $V - A$ mixing vertex

In this section, we show that the metric tensor part of the two-point functions for the $V - A$ mixing satisfies the relation in Eq.(68). Multiplying Eq.(67) by O_V^T , one can find,

$$\begin{aligned}\Pi^{VA} &= O_V^T \Pi^{V^0A} \\ &= -\frac{1}{g} \begin{pmatrix} M_\rho^2 O_{V11} + M_{V\rho 8}^2 O_{V21} + M_{V0\rho}^2 O_{V31} + \frac{M_{V\rho 8}^2 O_{V11} + M_{V88}^2 O_{V21} + M_{V08}^2 O_{V31}}{\sqrt{3}} \\ M_\rho^2 O_{V12} + M_{V\rho 8}^2 O_{V22} + M_{V0\rho}^2 O_{V32} + \frac{M_{V\rho 8}^2 O_{V12} + M_{V88}^2 O_{V22} + M_{V08}^2 O_{V32}}{\sqrt{3}} \\ M_\rho^2 O_{V13} + M_{V\rho 8}^2 O_{V23} + M_{V0\rho}^2 O_{V33} + \frac{M_{V\rho 8}^2 O_{V13} + M_{V88}^2 O_{V23} + M_{V08}^2 O_{V33}}{\sqrt{3}} \end{pmatrix}.\end{aligned}\quad (D1)$$

Meanwhile, the diagonalization of the mass matrix leads,

$$\begin{pmatrix} M_\rho^2 & M_{V\rho 8}^2 & M_{V0\rho}^2 \\ M_{V\rho 8}^2 & M_{V88}^2 & M_{V08}^2 \\ M_{V0\rho}^2 & M_{V08}^2 & M_{0V}^2 \end{pmatrix} O_V = O_V \begin{pmatrix} \mathcal{M}_1^2 & 0 & 0 \\ 0 & \mathcal{M}_2^2 & 0 \\ 0 & 0 & \mathcal{M}_3^2 \end{pmatrix}. \quad (\text{D2})$$

In the above equation, the matrix elements for $(i, j) = (1, I), (2, I)$ indicate the following relations,

$$M_\rho^2 O_{V1I} + M_{V\rho 8}^2 O_{V2I} + M_{V0\rho}^2 O_{V3I} = \mathcal{M}_I^2 O_{V1I}, \quad (\text{D3})$$

$$M_{V\rho 8}^2 O_{V1I} + M_{V88}^2 O_{V2I} + M_{V08}^2 O_{V3I} = \mathcal{M}_I^2 O_{V2I}. \quad (\text{D4})$$

Plugging Eqs.(D3, D4) into Eq.(D1), one can find that the relation in Eq.(68) is satisfied.

Appendix E: 1-loop correction to self-energy of charged pseudoscalars

In this appendix, the radiative correction to charged pseudoscalar masses is discussed. Background field method is used to evaluate the chiral loop correction[34, 35]. Kinetic terms and 1-loop corrected masses in effective Lagrangian are given as,

$$\mathcal{L}_{\text{eff}} = \sum_P^{\pi^+, K^+, K^0} \left(\frac{1}{Z_P} \partial_\mu P_f \partial^\mu \bar{P}_f - M_P^2 P_f \bar{P}_f \right) \quad (\text{E1})$$

$$= \sum_P^{\pi^+, K^+, K^0} (\partial_\mu P \partial^\mu \bar{P} - M_P^2 P \bar{P}). \quad (\text{E2})$$

In Eq.(E1), we denote P_f as the pseudoscalar in original flavor basis and the coefficient of the kinetic term is,

$$\frac{1}{Z_P} = 1 - Z_{P(1)}, \quad (\text{E3})$$

$$Z_{\pi^+(1)} \sim -8 \left(\frac{M_{\pi^+}^2 + 2\bar{M}_K^2}{f^2} L_4^r + \frac{M_{\pi^+}^2}{f^2} L_5^r \right) + 2c(2\mu_{\pi^+} + \bar{\mu}_K), \quad (\text{E4})$$

$$Z_{K^+(1)} \simeq Z_{K^0(1)} \sim -8 \left(\frac{M_{\pi^+}^2 + 2\bar{M}_K^2}{f^2} L_4^r + \frac{\bar{M}_K^2}{f^2} L_5^r \right) + c \left(\frac{3}{2}\mu_{\pi^+} + \frac{3}{2}\mu_{88} + 3\bar{\mu}_K \right). \quad (\text{E5})$$

In Eq.(E1), normalization of the kinetic term is slightly deviated from unity due to 1-loop correction. In order to canonically normalize Z_P in Eq.(E1), one should implement the transformation in the following form as,

$$P_f^{(-)} = \sqrt{Z_P^{(-)}} P, \quad (\text{E6})$$

$$\sqrt{Z_P} \sim 1 + \frac{Z_{P(1)}}{2}. \quad (\text{E7})$$

Using transformation in Eq.(E6), one obtains Lagrangian in Eq.(E2). We keep linear order of the small quantities (i.e., we neglect quadratic terms with respect to isospin breaking and 1-loop correction multiplied by isospin violation). The masses in Eq.(E2) are,

$$M_{\pi^+}^{\prime 2} \simeq (M_{\pi^+}^2)_{\text{tr}} \left[1 + (4c - 3)\mu_{\pi^+} - \frac{1}{3}\mu_{88} + 2(c - 1)\bar{\mu}_K \right. \\ \left. - 8\frac{M_{\pi^+}^2 + 2\bar{M}_K^2}{f^2}L_{46}^r - 8\frac{M_{\pi^+}^2}{f^2}L_{58}^r \right] + \Delta_{\text{EM}}, \quad (\text{E8})$$

$$M_{K^+}^{\prime 2} \simeq (M_{K^+}^2)_{\text{tr}} \left[1 + \frac{3}{2}(c - 1)\mu_{\pi^+} + \frac{1}{6}(9c - 5)\mu_{88} + 3(c - 1)\bar{\mu}_K \right. \\ \left. - 8\frac{M_{\pi^+}^2 + 2\bar{M}_K^2}{f^2}L_{46}^r - 8\frac{\bar{M}_K^2}{f^2}L_{58}^r \right] + \Delta_{\text{EM}}, \quad (\text{E9})$$

$$M_{K^0}^{\prime 2} \simeq (M_{K^0}^2)_{\text{tr}} \left[1 + \frac{3}{2}(c - 1)\mu_{\pi^+} + \frac{1}{6}(9c - 5)\mu_{88} + 3(c - 1)\bar{\mu}_K \right. \\ \left. - 8\frac{M_{\pi^+}^2 + 2\bar{M}_K^2}{f^2}L_{46}^r - 8\frac{\bar{M}_K^2}{f^2}L_{58}^r \right], \quad (\text{E10})$$

where low energy constants are denoted as,

$$L_{46}^r = L_4^r - 2L_6^r, \quad L_{58}^r = L_5^r - 2L_8^r, \quad \Delta_{\text{EM}} = \frac{2C}{9f^2}. \quad (\text{E11})$$

In Eqs.(E8-E10), $(M_P^2)_{\text{tr}}$ denotes the tree level mass parameters, and in the loop corrections, pseudoscalar masses are identified with physical masses expressed as $M_{\pi^+}^2$ and \bar{M}_K^2 defined in Eq.(30) since their difference gives rise to minor correction in Eqs.(E8-E10). The tree level mass parameters in r.h.s. of Eqs.(E8-E10) are given as Gell-Mann-Oakes-Renner (GMOR) relation,

$$(M_{\pi^+}^2)_{\text{tr}} = \frac{2B(m_u + m_d)}{f^2}, \quad (M_{K^+}^2)_{\text{tr}} = \frac{2B(m_u + m_s)}{f^2}, \quad (M_{K^0}^2)_{\text{tr}} = \frac{2B(m_d + m_s)}{f^2}. \quad (\text{E12})$$

One can clarify that the 1-loop masses are renormalization scale invariant, i.e., the following equation is satisfied,

$$\frac{\partial M_{\pi^+}^{\prime 2}}{\partial \ln \mu} = \frac{\partial M_{K^+}^{\prime 2}}{\partial \ln \mu} = \frac{\partial M_{K^0}^{\prime 2}}{\partial \ln \mu} = 0. \quad (\text{E13})$$

Appendix F: 1-loop correction to self-energy of neutral pseudoscalars

In this appendix, the radiative correction to pseudoscalar masses is estimated for neutral particles. As analogous to the previous section, the background field method is used to

evaluate the quantum correction. We consider the framework in which chiral octet loop correction is taken into account. Masses and kinetic terms of pseudoscalars in 1-loop corrected effective Lagrangian are described as,

$$\mathcal{L}_{\text{eff}} = \frac{1}{2}(\partial_\mu \pi_3, \partial_\mu \eta_8, \partial_\mu \eta_0) \frac{1}{Z} (\partial^\mu \pi_3, \partial^\mu \eta_8, \partial^\mu \eta_0)^T - \frac{1}{2}(\pi_3, \eta_8, \eta_0) M^2 (\pi_3, \eta_8, \eta_0)^T \quad (\text{F1})$$

(SU(3) eigenstate)

$$= \frac{1}{2} \partial_\mu \pi_3^R \partial^\mu \pi_3^R + \frac{1}{2} \partial_\mu \eta_8^R \partial^\mu \eta_8^R + \frac{1}{2} \partial_\mu \eta_0^R \partial^\mu \eta_0^R - \frac{1}{2} (\pi_3^R, \eta_8^R, \eta_0^R) M'^2 (\pi_3^R, \eta_8^R, \eta_0^R)^T \quad (\text{F2})$$

(kinetic terms rescaled)

$$= \frac{1}{2} \partial_\mu \pi^0 \partial^\mu \pi^0 + \frac{1}{2} \partial_\mu \eta \partial^\mu \eta + \frac{1}{2} \partial_\mu \eta' \partial^\mu \eta' - \frac{1}{2} (\pi^0, \eta, \eta') \text{diag}(M_{\pi^0}^2, M_\eta^2, M_{\eta'}^2) (\pi^0, \eta, \eta')^T. \quad (\text{F3})$$

(mass eigenstate)

In Eq.(F1), the coefficient of kinetic terms is given as a 3×3 matrix,

$$\frac{1}{Z} \simeq \begin{pmatrix} 1 - Z_{33(1)} & 0 & 0 \\ 0 & 1 - Z_{88(1)} & 0 \\ 0 & 0 & 1 \end{pmatrix}, \quad (\text{F4})$$

$$Z_{33(1)} \sim Z_{\pi^+(1)}, \quad (\text{F5})$$

$$Z_{88(1)} = -8 \left(\frac{M_{\pi^+}^2 + 2M_{\bar{K}}}{f^2} L_4^r + \frac{M_{88}^2}{f^2} L_5^r \right) + 6c\mu_{\bar{K}}. \quad (\text{F6})$$

The matrix in Eq.(F4) implies that the kinetic terms in Eq.(F1) are slightly deviated from unity with 1-loop correction. The mass matrix denoted as M^2 in Eq.(F1) indicates the 1-loop corrected mixing mass matrix in the SU(3) basis. To normalize the kinetic terms in Eq.(F1) canonically, one should implement basis transformation,

$$\begin{pmatrix} \pi_3 \\ \eta_8 \\ \eta_0 \end{pmatrix} = \sqrt{Z} \begin{pmatrix} \pi_3^R \\ \eta_8^R \\ \eta_0^R \end{pmatrix}, \quad \sqrt{Z} \sim \begin{pmatrix} \sqrt{Z_1^\pi} & 0 & 0 \\ 0 & \sqrt{Z_2^\pi} & 0 \\ 0 & 0 & 1 \end{pmatrix}, \quad (\text{F7})$$

$$\sqrt{Z_1^\pi} = 1 + \frac{Z_{33(1)}}{2} \sim \sqrt{Z_{\pi^+}}, \quad (\text{F8})$$

$$\sqrt{Z_2^\pi} = 1 + \frac{Z_{88(1)}}{2}. \quad (\text{F9})$$

The transformation in Eq.(F7) relates the basis in Eq.(F1) to one given in Eq.(F2). Thus, the kinetic terms are canonically normalized in Eqs.(F2-F3). One diagonalizes the mass matrix in Eq.(F2) and obtains Lagrangian with mass eigenstates in Eq.(F3). The mass

matrix given in Eq.(F2) is expressed as,

$$M'^2 = \begin{pmatrix} M'_{33}{}^2 & M'_{38}{}^2 & M'_{30}{}^2 \\ * & M'_{88}{}^2 & M'_{80}{}^2 \\ * & * & M'_{00}{}^2 \end{pmatrix}. \quad (\text{F10})$$

In the above mass matrix, the 1-loop corrected masses are denoted with primes attached. We adopt the same approximation as the charged pseudoscalars, i.e., ignore quadratic terms with respect to the small quantities so that the 1-loop corrected masses in Eq.(F10) are simplified as,

$$M'_{33}{}^2 \simeq (M_{\pi^+}^2)_{\text{tr}} \left[1 + (4c - 3)\mu_{\pi^+} - \frac{1}{3}\mu_{88} + 2(c - 1)\bar{\mu}_K - 8\frac{M_{\pi^+}^2 + 2\bar{M}_K^2}{f^2}L_{46}^r - 8\frac{M_{\pi^+}^2}{f^2}L_{58}^r \right], \quad (\text{F11})$$

$$M'_{38}{}^2 \simeq M_{38}^2 = \frac{(M_{K^+}^2)_{\text{tr}} - (M_{K^0}^2)_{\text{tr}}}{\sqrt{3}}, \quad (\text{F12})$$

$$M'_{88}{}^2 \simeq M_{88}^2 - M_{\pi^+}^2\mu_{\pi^+} - \left(\frac{16\bar{M}_K^2 - 7M_{\pi^+}^2}{9} \right) \mu_{88} + \frac{2}{3} (9cM_{88}^2 + 3M_{\pi^+}^2 - 8\bar{M}_K^2) \bar{\mu}_K - \frac{8M_{88}^2}{f^2} (M_{\pi^+}^2 + 2\bar{M}_K^2) L_{46}^r - \frac{8}{f^2} M_{88}^4 L_5^r + \frac{16}{3f^2} [8(M_{\pi^+}^2 - \bar{M}_K^2)^2 L_7^r + (M_{\pi^+}^4 + 2(M_{\pi^+}^2 - 2\bar{M}_K^2)^2) L_8^r], \quad (\text{F13})$$

$$M'_{30}{}^2 \simeq M_{30}^2 = -\hat{g}_{2p} [(M_{K^+}^2)_{\text{tr}} - (M_{K^0}^2)_{\text{tr}}], \quad (\text{F14})$$

$$M'_{80}{}^2 \simeq M_{80}^2 + \frac{\hat{g}_{2p}}{\sqrt{3}} \left[3M_{\pi^+}^2\mu_{\pi^+} + \frac{1}{3} (5M_{\pi^+}^2 - 8\bar{M}_K^2) \mu_{88} + 2 \{ 3c(M_{\pi^+}^2 - \bar{M}_K^2) + (3M_{\pi^+}^2 - 4\bar{M}_K^2) \} \bar{\mu}_K \right] - 2M_{80}^2 \left[\frac{M_{\pi^+}^2 + 2\bar{M}_K^2}{f^2} T_{34}^r - \frac{2\bar{M}_K^2}{f^2} T_5^r + \frac{2M_{88}^2}{f^2} L_5^r \right], \quad (\text{F15})$$

where $T_{34}^r = 2L_4^r - T_3^r$ and $\hat{g}_{2p} = fg_{2p}/B$. 1-loop masses in Eqs.(F11-F15) are invariant under renormalization, hence they satisfy the following relation,

$$\frac{\partial M'_{33}{}^2}{\partial \ln \mu} = \frac{\partial M'_{38}{}^2}{\partial \ln \mu} = \frac{\partial M'_{88}{}^2}{\partial \ln \mu} = \frac{\partial M'_{30}{}^2}{\partial \ln \mu} = \frac{\partial M'_{80}{}^2}{\partial \ln \mu} = 0. \quad (\text{F16})$$

Comparing Eqs.(E8-E10) with Eqs.(F11, F12, F14), one finds that the neutral mass matrix elements are related to charged ones as,

$$M'_{33}{}^2 \sim M_{\pi^+}^2 - \Delta_{\text{EM}}, \quad (\text{F17})$$

$$M'_{38}{}^2 \sim \frac{1}{\sqrt{3}} (M_{K^+}^2 - M_{K^0}^2 - \Delta_{\text{EM}}), \quad (\text{F18})$$

$$M'_{30}{}^2 \sim -\hat{g}_{2p} (M_{K^+}^2 - M_{K^0}^2 - \Delta_{\text{EM}}). \quad (\text{F19})$$

The mixing matrix should be determined to diagonalize the mass matrix as,

$$O^T M'^2 O = \text{diag}(M_{\pi^0}^2, M_{\eta}^2, M_{\eta'}^2). \quad (\text{F20})$$

Appendix G: 1-loop correction to decay constants of π^+ and K^+

In this appendix, 1-loop corrected decay constants are analyzed for charged pseudoscalars. The decay constants are defined with parameterizing matrix elements as,

$$\langle \pi^+(p) | \bar{u} \gamma_\mu \gamma_5 d | 0 \rangle |_{1\text{-loop order}} = i\sqrt{2} f_{\pi^+} p_\mu, \quad (\text{G1})$$

$$\langle K^+(p) | \bar{u} \gamma_\mu \gamma_5 s | 0 \rangle |_{1\text{-loop order}} = i\sqrt{2} f_{K^+} p_\mu. \quad (\text{G2})$$

One can find that 1-loop corrected decay constants are related with wave function renormalization in Eq.(E6) in the following as,

$$f_{\pi^+} = \frac{f}{\sqrt{Z_{\pi^+}}}, \quad f_{K^+} = \frac{f}{\sqrt{Z_{K^+}}}, \quad (\text{G3})$$

where one can show that the quantities in Eq.(G3) are renormalization scale invariant, i.e.,

$$\frac{\partial}{\partial \ln \mu} f_{\pi^+} = \frac{\partial}{\partial \ln \mu} f_{K^+} = 0. \quad (\text{G4})$$

Equation(G3) leads to the relation between the decay constants of pion and one for kaon in Eq.(73).

Appendix H: Wess-Zumino-Witten term

In this appendix, we give the expression for the WZW term. The WZW term is obtained by integrating the Bardeen form anomaly as suggested in Ref.[7]. Following Ref.[20], we write down the expression for the WZW term as,

$$\begin{aligned} \mathcal{L}_{\text{WZ}} = & -\frac{N_c}{16\pi^2} \epsilon^{\mu\nu\rho\sigma} \int_0^1 dt \text{tr} \frac{\pi}{f} \left[V_{\mu\nu}(t) V_{\rho\sigma}(t) + \frac{1}{3} A_{\mu\nu}(t) A_{\rho\sigma}(t) \right. \\ & - \frac{8i}{3} (V_{\mu\nu}(t) A_\rho(t) A_\sigma(t) + A_\mu(t) V_{\nu\rho}(t) A_\sigma(t) + A_\mu(t) A_\nu(t) V_{\rho\sigma}(t)) \\ & \left. - \frac{32}{3} A_\mu(t) A_\nu(t) A_\rho(s) A_\sigma(t) \right]. \end{aligned} \quad (\text{H1})$$

In Eq.(H1), $N_c = 3$ shows the color factor and the notations are defined as,

$$V_\mu(t) = \frac{1}{2}(\xi(t)V_\mu\xi(-t) + \xi(-t)V_\mu\xi(t) + \xi(t)A_\mu\xi(-t) - \xi(-t)A_\mu\xi(t) - i\xi(t)\partial_\mu\xi(-t) - i\xi(-t)\partial_\mu\xi(t)), \quad (\text{H2})$$

$$A_\mu(t) = \frac{1}{2}(\xi(t)V_\mu\xi(-t) - \xi(-t)V_\mu\xi(t) + \xi(t)A_\mu\xi(-t) + \xi(-t)A_\mu\xi(t) - i\xi(t)\partial_\mu\xi(-t) + i\xi(-t)\partial_\mu\xi(t)), \quad (\text{H3})$$

$$V_{\mu\nu}(t) = \partial_\mu V_\nu(t) - \partial_\nu V_\mu(t) + i[V_\mu(t), V_\nu(t)] + i[A_\mu(t), A_\nu(t)], \quad (\text{H4})$$

$$A_{\mu\nu}(t) = \partial_\mu A_\nu(t) - \partial_\nu A_\mu(t) + i[V_\mu(t), A_\nu(t)] + i[A_\mu(t), V_\nu(t)], \quad (\text{H5})$$

$$\xi(t) = e^{-i(1-t)\pi/f}. \quad (\text{H6})$$

The expressions given in Eqs.(H1-H6) are all defined in Minkowski space-time.

-
- [1] R. Arnaldi *et al.* [NA60 Collaboration], Phys. Lett. B **757**, 437 (2016).
doi:10.1016/j.physletb.2016.04.013
 - [2] M. Ablikim *et al.* [BESIII Collaboration], Phys. Rev. D **92**, no. 1, 012001 (2015)
doi:10.1103/PhysRevD.92.012001 [arXiv:1504.06016 [hep-ex]].
 - [3] M. Bando, T. Kugo, S. Uehara, K. Yamawaki and T. Yanagida, Phys. Rev. Lett. **54**, 1215 (1985). doi:10.1103/PhysRevLett.54.1215
 - [4] G. Ecker, J. Gasser, A. Pich and E. de Rafael, Nucl. Phys. B **321**, 311 (1989).
doi:10.1016/0550-3213(89)90346-5
 - [5] G. Ecker, J. Gasser, H. Leutwyler, A. Pich and E. de Rafael, Phys. Lett. B **223**, 425 (1989).
doi:10.1016/0370-2693(89)91627-4
 - [6] G. C. Wick, A. S. Wightman and E. P. Wigner, Phys. Rev. **88**, 101 (1952).
doi:10.1103/PhysRev.88.101
 - [7] J. Wess and B. Zumino, Phys. Lett. B **37**, 95 (1971).
 - [8] E. Witten, Nucl. Phys. B **223**, 422 (1983). doi:10.1016/0550-3213(83)90063-9
 - [9] T. Fujiwara, T. Kugo, H. Terao, S. Uehara and K. Yamawaki, Prog. Theor. Phys. **73**, 926 (1985).
 - [10] M. Bando, T. Kugo and K. Yamawaki, Phys. Rept. **164**, 217 (1988).
 - [11] A. Bramon, A. Grau and G. Pancheri, Phys. Lett. B **344**, 240 (1995). doi:10.1016/0370-2693(94)01543-L

- [12] M. Hashimoto, Phys. Rev. D **54**, 5611 (1996) doi:10.1103/PhysRevD.54.5611 [hep-ph/9605422].
- [13] C. Terschlusen and S. Leupold, Phys. Lett. B **691**, 191 (2010) doi:10.1016/j.physletb.2010.06.033 [arXiv:1003.1030 [hep-ph]].
- [14] C. Terschlusen, S. Leupold and M. F. M. Lutz, Eur. Phys. J. A **48**, 190 (2012) doi:10.1140/epja/i2012-12190-6 [arXiv:1204.4125 [hep-ph]].
- [15] S. P. Schneider, B. Kubis and F. Niecknig, Phys. Rev. D **86**, 054013 (2012) doi:10.1103/PhysRevD.86.054013 [arXiv:1206.3098 [hep-ph]].
- [16] Y. H. Chen, Z. H. Guo and H. Q. Zheng, Phys. Rev. D **85**, 054018 (2012) doi:10.1103/PhysRevD.85.054018 [arXiv:1201.2135 [hep-ph]].
- [17] A. Bramon, R. Escribano and M. D. Scadron, Phys. Lett. B **503**, 271 (2001) doi:10.1016/S0370-2693(01)00161-7 [hep-ph/0012049].
- [18] D. Kimura, K. Y. Lee and T. Morozumi, PTEP **2013**, 053B03 (2013) [Erratum-ibid. **2014**, no. 8, 089202 (2014)] [arXiv:1201.1794 [hep-ph]].
- [19] R. Urech, Nucl. Phys. B **433**, 234 (1995) [hep-ph/9405341].
- [20] K. Fujikawa and H. Suzuki, Oxford, UK: Clarendon (2004) 284 p
- [21] T. D. Lee and C. N. Yang, Nuovo Cim. **10**, 749 (1956).
- [22] A. Pilaftsis and C. E. M. Wagner, Nucl. Phys. B **553**, 3 (1999) [hep-ph/9902371].
- [23] K.A. Olive *et al.* [Particle Data Group], Chin. Phys. C **38**, 090001 (2014)
- [24] M. N. Achasov *et al.*, J. Exp. Theor. Phys. **107**, 61 (2008). doi:10.1134/S1063776108070054
- [25] R. I. Dzhelyadin *et al.*, Phys. Lett. B **102**, 296 (1981) [JETP Lett. **33**, 228 (1981)]. doi:10.1016/0370-2693(81)90879-0
- [26] R. R. Akhmetshin *et al.* [CMD-2 Collaboration], Phys. Lett. B **613**, 29 (2005) doi:10.1016/j.physletb.2005.03.019 [hep-ex/0502024].
- [27] D. Babusci *et al.* [KLOE-2 Collaboration], Phys. Lett. B **742**, 1 (2015) doi:10.1016/j.physletb.2015.01.011 [arXiv:1409.4582 [hep-ex]].
- [28] M. N. Achasov *et al.*, Phys. Lett. B **504**, 275 (2001). doi:10.1016/S0370-2693(01)00320-3
- [29] A. Anastasi *et al.* [KLOE-2 Collaboration], arXiv:1601.06565 [hep-ex].
- [30] P. Adlarson *et al.* [WASA-at-COSY Collaboration], Phys. Lett. B **707**, 243 (2012) doi:10.1016/j.physletb.2011.12.027 [arXiv:1107.5277 [nucl-ex]].

- [31] R. I. Dzhelyadin *et al.*, Phys. Lett. B **94**, 548 (1980) [Sov. J. Nucl. Phys. **32**, 516 (1980)] [Yad. Fiz. **32**, 998 (1980)]. doi:10.1016/0370-2693(80)90937-5
- [32] P. Aguar-Bartolome *et al.* [A2 Collaboration], Phys. Rev. C **89**, no. 4, 044608 (2014) doi:10.1103/PhysRevC.89.044608 [arXiv:1309.5648 [hep-ex]].
- [33] R. I. Dzhelyadin *et al.*, Sov. J. Nucl. Phys. **32**, 520 (1980) [Yad. Fiz. **32**, 1005 (1980)].
- [34] J. F. Donoghue, E. Golowich and B. R. Holstein, Camb. Monogr. Part. Phys. Nucl. Phys. Cosmol. **2**, 1 (1992).
- [35] J. Gasser and H. Leutwyler, Nucl. Phys. B **250**, 465 (1985). doi:10.1016/0550-3213(85)90492-4